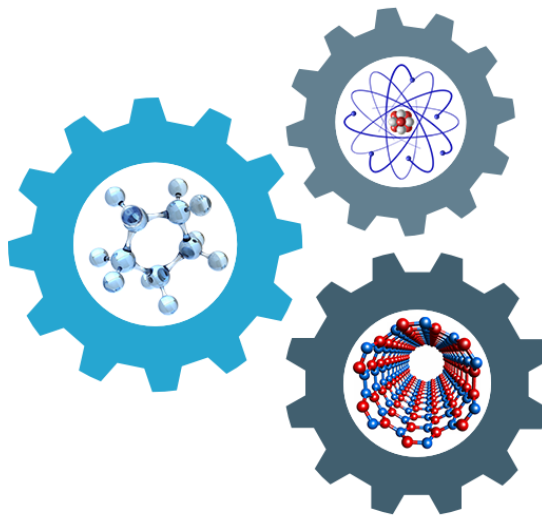


# **CONFERENCE PROGRAMME and BOOK OF ABSTRACTS**



**3<sup>rd</sup> International Conference on  
Innovative Materials and NanoEngineering  
(IMNE'2023)**

**November 10-13, 2023  
Dovgoluka, Ukraine**



## TABLE OF CONTENT

|   |    |
|---|----|
| Conference Organizers .....                       | 5  |
| Welcoming Message from the Conference Chair ..... | 7  |
| Travel Arrangement .....                          | 9  |
| Organizing Committee .....                        | 11 |
| International Program Committee .....             | 12 |
| Conference Program Agenda .....                   | 13 |
| Plenary Session .....                             | 15 |
| List of Presentations.....                        | 15 |
| Sponsors .....                                    | 20 |

## BOOK OF ABSTRACTS

|   |    |
|---|----|
| Content .....   | 23 |
| Section 1 .....   | 27 |
| <i>INNOVATIVE MATERIALS</i>   |    |
| Section 2 .....   | 37 |
| <i>OPTICAL AND QUASIOPTICAL TECHNIQUES FOR MATERIALS<br/>CHARACTERIZATION</i> |    |
| Section 3 .....   | 53 |
| <i>NANOENGINEERING TECHNOLOGIES AND PROCESSES</i>                             |    |
| Section 4 .....   | 63 |
| <i>APPLICATIONS OF INNOVATIVE MATERIALS</i>                                   |    |



## ORGANIZED BY



**Center of Excellence for Innovative Technologies and NanoEngineering,  
Department of Applied Physics and Nanomaterials Science**

Lviv Polytechnic National University  
5 Knyazya Romana Str., office 235  
79005, Lviv, Ukraine



**Faculty of Electrical Engineering**

Czestochowa University of Technology  
69 Dabrowskiego Str.,  
42-201, Czestochowa, Poland



**Institute of Sciences and Molecular Technologies of Angers**

University of Angers  
40 Rue de Rennes, Angers Cedex 01,  
49035, FRANCE



**Sub-Terahertz Technology Division  
Institute of Radioelectronics and Multimedia Technology**

Warsaw University of Technology  
Nowowiejska 15/19  
00-665 Warsaw, Poland



**Private Enterprise Softpartners**

97 Yevhena Konovaltsja Str.,  
79057 Lviv, Ukraine

## **IN TECHNICAL CO-SPONSORSHIP**



This conference has received funding from the European Union's Horizon 2020 research and innovation programme under the Marie Skłodowska-Curie grant agreement No 778156

## Welcoming Message from the Conference Chairman



Dear Colleagues,

With great pride and anticipation, I extend a warm welcome to all participants of the 3rd International Conference on Innovative Materials and NanoEngineering (IMNE'2023). As we gather once again, this year's location offers a backdrop of tranquility amidst the picturesque foot of the Carpathian Mountains, situated in the Relax Complex "Shepilske Urochishche," Dovgoluka village, Stryi District, Lviv Region, Ukraine.

As with our previous conference, due to the ongoing full-scale Russian war against Ukraine, we are forced to hold this conference in Ukraine. The Russian invasion of Ukraine has been a deeply distressing and tragic event in contemporary history. The incursion has led to immense humanitarian consequences, with countless innocent lives lost, displacement of civilians, and widespread destruction of infrastructure. Beyond the tangible damage, the invasion has instilled fear and anxiety among the Ukrainian people, who have had to endure the sounds of bombings, the sight of armed troops, and the uncertainty of what each day might bring. However, we remain hopeful for a peaceful resolution and the resurgence of Ukrainian science and society.

This year, we're adapting with a hybrid conference format, allowing for a broader spectrum of participation from esteemed scientists across Ukraine, Poland, Germany, France, and other EU countries. This amalgamation of minds, supported by the European Union's IMAGE project No. 778156 (H2020-MSCA-RISE-2017 program), aims to foster a deeper understanding and collaboration in the realm of innovative materials and nanoengineering.

The IMNE conference is a melting pot of ideas, innovations, and potential collaborations, especially in manufacturing, optical, and quasi-optical research of pioneering materials and emerging nanotechnologies. Our diverse attendees, comprising academic luminaries, industry leaders, and pioneers from the private sector, have the unique opportunity to both present and absorb groundbreaking scientific and technological advancements, propelling their endeavors to new heights.

Our mission extends beyond mere presentations. We envision spirited discussions around the challenges, prospects, and practical implementations in the fields of micro- and nanoelectronics. Rest assured, our dedicated organizing committee has left no stone unturned to ensure this conference aligns with the highest international standards.

**“Innovative Materials and NanoEngineering” (IMNE'2023)  
November 10-13, 2023, Dovgoluka, Ukraine**

In conclusion, as we embark on this intellectual journey, I hope that IMNE'2023 serves as a catalyst for fresh insights and enduring collaborations. On behalf of the entire organizing committee, I congratulate each one of you for being a part of this grand endeavor and wish you an enlightening experience at IMNE'2023.

*Warm regards,*

*Anatoliy Andrushchak*

*IMNE Conference Chairman*

<https://imne.lpnu.ua>

## TRAVEL ARRANGEMENT

The IMNE-2023 conference is scheduled to take place in Dovholuka village, Stryi district, within the Lviv region of Ukraine. For transportation convenience, the organizers are considering the provision of shuttle services for groups. However, participants are advised to liaise with the organizing committee in advance to ensure arrangements.

Delegates will be accommodated at the Relax Complex "Shepilska," strategically situated amidst the Carpathians, nestled between the renowned Morshyn and Truskavets resorts. This venue is optimal for relaxation and conducive for scholarly conferences. The complex is situated in a serene setting alongside Lake Shepilska and is a mere 20-minute drive from Stryi. The accommodation at "Shepilska" boasts rooms adorned in subtle hues, while the cottages are gracefully finished with wood. Additionally, the on-site restaurant at the Shepilska complex offers a delectable blend of Ukrainian and European cuisines for guests to relish.

### HOTEL ADDRESS

#### Relax Complex Shepilska

Urochische Shepil'ske 1, Dovgoluka, Lviv region  
Ukraine

**Telephone:** 095 260 50 10

**Telephone:** 098 342 18 00

**Website:** <https://shepilska.com.ua/>





## ORGANIZING COMMITTEE

|                  |   |
|------------------|---|
| <b>Chairman:</b> | <b>Prof. Anatoliy Andrushchak,</b><br>Lviv Polytechnic National University, UKRAINE |
|------------------|---|

|                       |  |
|-----------------------|--|
| <b>Vice-chairmen:</b> | <b>Prof. Andriy Kityk,</b><br>Czestochowa University of Technology,<br>POLAND<br><br><b>Prof. Bouchta Sahraoui</b><br>University of Angers,<br>FRANCE<br><br><b>Prof. Yevhen Yashchyshyn</b><br>Warsaw University of Technology,<br>POLAND |
|-----------------------|--|

|                              |  |
|------------------------------|--|
| <b>Conference Secretary:</b> | <b>Dr. Nazariy Andrushchak,</b><br>Lviv Polytechnic National University,<br>Private Enterprise Softpartners, UKRAINE |
|------------------------------|--|

|                           |  |
|---------------------------|--|
| <b>Publication Chair:</b> | <b>Dr. Nazariy Andrushchak,</b><br>Lviv Polytechnic National University,<br>Private Enterprise Softpartners, UKRAINE |
|---------------------------|--|

## MEMBERS OF THE ORGANIZING COMMITTEE

|                           |   |
|---------------------------|---|
| <b>Dr. Bohdan Venhryn</b> | Lviv Polytechnic National University, UKRAINE |
| <b>Dr. Oksana Balaban</b> | Lviv Polytechnic National University, UKRAINE |
| <b>Andrii Danylov</b>     | Lviv Polytechnic National University, UKRAINE |
| <b>Dr. Zinoviy Kogut</b>  | Lviv Polytechnic National University, UKRAINE |
| <b>Dr. Roman Shvets</b>   | Lviv Polytechnic National University, UKRAINE |
| <b>Dr. Andrii Bendak</b>  | Lviv Polytechnic National University, UKRAINE |

## INTERNATIONAL PROGRAM COMMITTEE

|                                 |   |
|---------------------------------|---|
| <b>Prof. Andrushchak A.</b>     | Lviv Polytechnic National University, UKRAINE<br><b>(Chairman)</b>                                  |
| <b>Prof. Adamiv V.</b>          | Vlokh Institute of Physical Optics Lviv, UKRAINE  |
| <b>Prof. Bryk T.</b>            | Institute for Condensed Matter Physics NAS,<br>UKRAINE  |
| <b>Prof. Buryy O.</b>           | Lviv Polytechnic National University, UKRAINE   |
| <b>Dr. Goering P.</b>           | SmartMembranes GmbH, GERMANY  |
| <b>Prof. Gogotsi Yu.</b>        | Drexel University, A.J. Drexel Nanomaterials<br>Institute, USA                                      |
| <b>Prof. Huber P.</b>           | Hamburg University of Technology, GERMANY   |
| <b>Dr. Sci. Ivashchyshyn F.</b> | Lviv Polytechnic National University, UKRAINE   |
| <b>Prof. Kityk A.</b>           | Czestochowa University of Technology, POLAND<br><b>(Vice-chairman)</b>                              |
| <b>Prof. Lukianets B.</b>       | Lviv Polytechnic National University, UKRAINE   |
| <b>Prof. Mytsyk B.</b>          | Karpenko Physico-Mechanical Institute of the<br>National Academy of Sciences of Ukraine,<br>UKRAINE |
| <b>Prof. Sahraoui B.</b>        | University of Angers, FRANCE <b>(Vice-chairman)</b>   |
| <b>Prof. Shchur Ya.</b>         | Institute for Condensed Matter Physics NAS Ukraine,<br>Private Enterprise SoftPartners, UKRAINE     |
| <b>Prof. Strelchuk V.</b>       | V.E. Lashkaryov Institute of Semiconductor Physics,<br>UKRAINE                                      |
| <b>Prof. Tkachuk V.</b>         | Ivan Franko National University of Lviv, UKRAINE  |
| <b>Prof. Vakiv M.</b>           | Scientific research company Carat – branch enterprise<br>of PJSC Concern-Electron (CARAT), Ukraine  |
| <b>Prof. Vitusevich S.</b>      | Forschungszentrum Julich GmbH, GERMANY  |
| <b>Prof. Yashchyshyn Ye.</b>    | Warsaw University of Technology, POLAND<br><b>(Vice-chairman)</b>                                   |

# 3<sup>rd</sup> International Conference on Innovative Materials and NanoEngineering (IMNE'2023)

## IMNE'2023 Conference Program Agenda

|                                    | Friday (November 10, 2023)   |
|------------------------------------|--|
| 13 <sup>00</sup> -15 <sup>00</sup> | Registration of participants   |
| 15 <sup>00</sup> -16 <sup>40</sup> | <b>Plenary Session</b><br>Chairman: <b>Prof. Anatoliy Andrushchak</b><br>Vice-chairman: <b>Dr. Nazariy Andrushchak</b> |
| 16 <sup>40</sup> -17 <sup>00</sup> | Coffee Break   |
| 17 <sup>00</sup> -19 <sup>00</sup> | <b>Session 1</b><br>Chairman: <b>Prof. Bouchta Sahraoui</b><br>Vice-chairman: <b>Prof. Oleh Buryy</b>                  |
| 19 <sup>00</sup> -22 <sup>00</sup> | Barbeque Dinner  |

|                                    | Saturday (November 11, 2023)   |
|------------------------------------|--|
| 10 <sup>00</sup> -12 <sup>00</sup> | <b>Session 2</b><br>Chairman: <b>Prof. Volodymyr Tkachuk</b><br>Vice-chairman: <b>Dr. Oksana Balaban</b> |
| 12 <sup>00</sup> -12 <sup>30</sup> | Coffee Break   |
| 13 <sup>30</sup> -14 <sup>30</sup> | Lunch time   |
| 14 <sup>30</sup> -18 <sup>00</sup> | <b>Session 3</b><br>Chairman: <b>Prof. Yaroslav Shchur</b><br>Vice-chairman: <b>Andriy Danylov</b>       |
| 16 <sup>15</sup> -16 <sup>45</sup> | Coffee Break   |
| 18 <sup>00</sup> -19 <sup>00</sup> | Scientific Discussions, Free time  |
| 19 <sup>00</sup> -22 <sup>00</sup> | Banquet  |

|                                    | Sunday (November 12, 2023)  |
|------------------------------------|---|
| 10 <sup>00</sup> -12 <sup>00</sup> | <b>Session 4</b><br>Chairman: <b>Prof. Yevhen Yashchyshyn</b><br>Vice-chairman: <b>Prof. Marian Kyryk</b> |
| 13 <sup>30</sup> -14 <sup>30</sup> | Lunch time  |

|                                       |  |
|---------------------------------------|--|
|                                       | <b>Monday (November 13, 2023)</b>      |
| <b>9<sup>00</sup>-11<sup>00</sup></b> | General Discussion, Conference Closing |

### **TIME OF PRESENTATIONS**

Oral presentation at the plenary session – 25 min.

Oral presentation at the regular session – 10 min.

Discussion, questions – up to 5 min.

**REGISTRATION**

**Friday, November 10**  
**13<sup>00</sup>-15<sup>00</sup>**

Registration of participants.

**PLENARY SESSION**

**Friday, November 10**  
**15<sup>00</sup>-16<sup>40</sup>**

**Chairman: Prof. Anatoliy Andrushchak**  
**Vice-chairman: Dr. Nazariy Andrushchak**

**SPEECH OF THE CONFERENCE ORGANIZER**

|                                    |   |
|------------------------------------|---|
| 15 <sup>00</sup> -15 <sup>10</sup> | <b>WELCOMING MESSAGE OF THE CONFERENCE CHAIRMAN</b><br><b>Head of Center of Excellence for Innovative Technologies and Nanoengineering at Lviv Polytechnic National University</b><br><i>Anatoliy Andrushchak</i> |
|------------------------------------|---|

**INVITED LECTURES**

|                                    |  |
|------------------------------------|--|
| 15 <sup>10</sup> -15 <sup>40</sup> | <b>Functionalised Selected Conjugated Compounds for Nonlinear Optical Applications</b><br><i>B. Sahraoui, H. Karout, A. A.V. Kityk, Y. Shchur, A. Andrushchak, R. Wielgosz, O. Kityk, M. Lelonek, P. Göring, O. Krupka</i>   |
| 15 <sup>40</sup> -16 <sup>10</sup> | <b>Silica-Benzil and Alumina-Benzil Crystalline Nanocomposites: Textural Morphology and Nonlinear Optical Characterization</b><br><i>A.V. Kityk, H. El Karout, B. Sahraoui, Y. Shchur, A. Andrushchak, R. Wielgosz, O. Kityk, J. Jędryka, Y. Slyvka, M. Lelonek, P. Göring, P. Huber</i> |
| 16 <sup>10</sup> -16 <sup>40</sup> | <b>Development of sub-THz Modulators. Experience and Results</b><br><i>Y. Yashchyshyn, V. Haiduchok, S. Krukowski, P. Bajurko, J. Sobolewski</i>   |

**SESSION 1**

**Friday, November 10**  
**17<sup>00</sup>-19<sup>00</sup>**

**Chairman: Prof. Bouchta Sahraoui**  
**Vice-chairman: Prof. Oleh Buryy**

|                                    |   |
|------------------------------------|---|
| 17 <sup>00</sup> -17 <sup>15</sup> | <b>In situ X-ray synchrotron diffraction as a tool for the study of structural and electronic instabilities of solids</b><br><i>L. Vasylechko, O. Pekinchak, O. Pavlovska, V. Hreb, A. Senyshyn</i>       |
| 17 <sup>15</sup> -17 <sup>30</sup> | <b>Mercury Detection Sensor Based on the Structure of Amorphous Se Film/Au Nanoparticles</b><br><i>M. Trunov, V. Rubish, V. Kyrylenko, M. Durkot</i>  |
| 17 <sup>30</sup> -17 <sup>45</sup> | <b>Formation of the Nanocrystalline Phase of Active Dielectrics on the Surface and in the Pores of Synthetic Opals</b><br><i>V. Moiseienko, M. Derhachov, B. Abu Sal</i>                                  |
| 17 <sup>45</sup> -18 <sup>00</sup> | <b>Generation of Acoustic Vortices and Acousto-Optic Interactions with Acoustic Vortex Beams</b><br><i>I. Martynyuk-Lototska, M. Kostyrko, D. Adamenko, I. Skab and R. Vlokh</i>                          |
| 18 <sup>00</sup> -18 <sup>15</sup> | <b>Optical Properties of Thin Film and Bulk Materials in the Visible and Infrared Spectrum Ranges</b><br><i>A. Danylov, D. Vynnyk, V. Haiduchok</i>   |
| 18 <sup>15</sup> -18 <sup>30</sup> | <b>Mesoporous Silica and Alumina as Efficient Supports for Solid Catalysts of Aldol Condensation Reaction</b><br><i>R. Nebesnyi, I. Demydov, S. Khalameida, V. Sydorchuk, V. Ivasiv</i>                   |
| 18 <sup>30</sup> -18 <sup>45</sup> | <b>Comparison of Series and Shunt GaN RF Switches for Millimeter-Wave Applications</b><br><i>P. Bajurko, J. Sobolewski, Y. Yashchyshyn</i>  |
| 18 <sup>45</sup> -19 <sup>00</sup> | <b>Effect of Photogeneration on Concentration of Excess Carriers in Si and Ge Crystals</b><br><i>A. Danylov, B. Venhryn, S. Luniov, A. Korolyshyn, I. Senko, D. Afanassyev, A. Ratych, A. Andrushchak</i> |

## SESSION 2

| Saturday, November 11<br>10 <sup>00</sup> -13 <sup>30</sup>   |   |
|---|---|
| <b>Chairman: Prof. Volodymyr Tkachuk</b><br><b>Vice-chairman: Dr. Oksana Balaban</b><br><br><b>INVITED LECTURES</b> |   |
| 10 <sup>00</sup> -10 <sup>30</sup>  | <b>Femtosecond Laser-Induced Periodic Surface Structures: Theory and Applications</b><br><i>I. Gnilitskyi</i> |

|                                    |  |
|------------------------------------|--|
| 10 <sup>30</sup> -11 <sup>00</sup> | <b>Multi-qubit Quantum Graph States and Studies of their Properties with Quantum Programming</b><br><i>Kh. Gnatenko</i>  |
| 11 <sup>00</sup> -11 <sup>30</sup> | <b>Computer Simulation Studies of Collective Dynamics in Complex Metallic Glasses and Ionic Melts</b><br><i>T. Bryk</i>  |
| <b>SESSION 2 PRESENTATIONS</b>     |  |
| 11 <sup>30</sup> -11 <sup>45</sup> | <b>Study of Relationship Between Nonlinear Optical Phenomena and the Molecular Structure of Specific Industrial Organic Compound</b><br><i>A. Aamoum, S. Taboukhat, A. Andrushchak, R. Wielgosz, M. Lelonek, P. Göring and B. Sahraoui</i> |
| 11 <sup>45</sup> -12 <sup>00</sup> | <b>Structures of InSb for Infrared Photodiodes Obtained by the Method of Pulsed Cooling of a Saturated Solution-Melt</b><br><i>M. Vakiv, S. Krukovskyi, I. Iznin, J. Kost, V. Arikov, O. Kulbachynskyi, O. Gudymienko, O. Dubikovskiy</i>  |
| 12 <sup>00</sup> -12 <sup>30</sup> | <b>Coffee Break</b>  |
| 12 <sup>30</sup> -12 <sup>45</sup> | <b>Supersymmetry and Entangled States in Quantum Optics</b><br><i>H. Laba, V. Tkachuk</i>  |
| 12 <sup>45</sup> -13 <sup>00</sup> | <b>Control of Second-Harmonic Generation via Phase-Matched induced by Magnetization in Iron Garnet Epitaxial Thin Films</b><br><i>I. Syvorotka, D. Guichaoua, N. Syvorotka, R. Wielgosz, A. Andrushchak, S. Taboukhat, B. Sahraoui</i>     |
| 13 <sup>00</sup> -13 <sup>15</sup> | <b>The Experimental Definition of Electro-optical Parameters in the LiTaO<sub>3</sub> Crystals. Analytical Representation of Spatial Anisotropy</b><br><i>B. Olkhovyk, Y. Lozynskyi, Z. Kohut</i>  |
| 13 <sup>15</sup> -13 <sup>30</sup> | <b>Silver-doped Lithium Triborate Glass for OSL Dosimetry</b><br><i>V. Adamiv, Ya. Burak, N. Volod'ko, U. Dutchak, T. Izo, I. Teslyuk, A. Luchechko</i>  |

### SESSION 3

|   |
|---|
| <p align="center"><b>Saturday, November 11</b><br/><b>14<sup>30</sup>-18<sup>00</sup></b></p> |
| <p><b>Chairman: Prof. Yaroslav Shchur</b><br/><b>Vice-chairman: Andriy Danylov</b></p>        |

## INVITED LECTURE

|                                    |   |
|------------------------------------|---|
| 14 <sup>30</sup> -15 <sup>00</sup> | <b>Quantum Computing of Physical Properties of Quantum Systems</b><br><i>H. Laba, V. Tkachuk</i>  |
| 15 <sup>00</sup> -15 <sup>30</sup> | <b>Why a Phosphor of the High Effective Atomic Number can be Useful for Dosimetry</b><br><i>S. Ubizskii, O. Poshvyak, Ya. Zhydachevskyy</i> |

## SESSION 3 PRESENTATIONS

|                                    |  |
|------------------------------------|--|
| 15 <sup>30</sup> -15 <sup>45</sup> | <b>Polymer-Containing Composites for Li<sup>+</sup> Intercalation Current Generation</b><br><i>O. Balaban, N. Mitina, A. Zaichenko, O. Izhyk</i>   |
| 15 <sup>45</sup> -16 <sup>00</sup> | <b>Comparative Investigation of Nonlinear Optical Responses in Various Lanthanide Coordination Compounds</b><br><i>H. El Karout, A.V. Kityk, R. Wielgosz, S. Taboukhat, D. Guichaoua, A. Andrushchak, O. Krupka and B. Sahraoui</i>                    |
| 16 <sup>00</sup> -16 <sup>15</sup> | <b>Topological Transition in Quasi 2D-crystals</b><br><i>B. Lukiyanets, D. Matulka</i>   |
| 16 <sup>15</sup> -16 <sup>45</sup> | <b>Coffee Break</b>  |
| 16 <sup>45</sup> -17 <sup>00</sup> | <b>Modeling the Separation Surface Influence on the Lattice Structure in Nanosystems</b><br><i>P. Kostrobii, I. Ryzha, M. Sheremeta</i>  |
| 17 <sup>00</sup> -17 <sup>15</sup> | <b>Photoelasticity of Ammonium Fluoroberylate Crystals</b><br><i>V. Stadnyk, B. Mytsyk, N. Demyanyshyn, P. Shchepanskyi, Y. Kost</i>   |
| 17 <sup>15</sup> -17 <sup>30</sup> | <b>Features of Photoelastic Properties of Ordered-structure Langasite Group Crystals</b><br><i>N. Demyanyshyn, B. Mytsyk, Yu. Maksishko, A. Erba, J. Maul, B. Olhovyk, O. Buryy, A. Andrushchak</i>  |
| 17 <sup>30</sup> -17 <sup>45</sup> | <b>Study of Coloumb Correlation Influence on SPPs Frequency Spectrum in Dielectric/Metal/Dielectric Structures</b><br><i>P. Kostrobii, V. Polovyi, O. Pits</i>   |
| 17 <sup>45</sup> -18 <sup>00</sup> | <b>Optical Properties Investigation of Nanoporous Al<sub>2</sub>O<sub>3</sub> Matrices with Embedded ADP and KB-5 Crystals</b><br><i>N. Andrushchak, D. Vynnyk, V. Haiduchok, A. Nikolenko, V. Adamiv, V. Strelchuk, O. Syrotynsky, A. Andrushchak</i> |

## SESSION 4

| Sunday, November 12<br>10 <sup>00</sup> -12 <sup>00</sup>                             |  |
|---|--|
| <b>Chairman: Prof. Yevhen Yashchyshyn</b><br><b>Vice-chairman: Prof. Marian Kyryk</b> |  |
| <b>INVITED LECTURES</b>   |  |
| 10 <sup>00</sup> -10 <sup>30</sup>  | <b>MXenes, Their Optical Properties and Interactions with Electromagnetic Waves</b><br><i>Y. Gogotsi</i>   |
| 10 <sup>30</sup> -11 <sup>00</sup>  | <b>Raman Spectroscopy and Symmetry Analysis in Structure Determining of Nanoconfined Nanocrystals</b><br><i>Ya. Shchur, A.V. Kityk, V. Adamiv, I. Teslyuk, S. Vitusevich, A. Andrushchak</i> |
| <b>SESSION 4 PRESENTATIONS</b>  |  |
| 11 <sup>00</sup> -11 <sup>15</sup>  | <b>The Optimal Geometries of Piezoelectric Effect in Trigonal Crystals</b><br><i>O. Buryy, M. Kyryk, A. Andrushchak</i>  |
| 11 <sup>15</sup> -11 <sup>30</sup>  | <b>Vector Phase Matching in Orthorhombic Biaxial Crystals by Extreme Surface Method</b><br><i>D. Shulha, O. Buryy, A. Andrushchak</i>  |
| 11 <sup>30</sup> -11 <sup>45</sup>  | <b>Selenium Thin Films Application in THz Range</b><br><i>A. Bendak, I. Senko, D. Vynnyk, V. Rubish</i>  |
| 11 <sup>45</sup> -12 <sup>00</sup>  | <b>Preparation of Bi<sub>12</sub>GeO<sub>20</sub> Nanocrystalline Structures</b><br><i>Ya. Shchur, V. Adamiv, I. Teslyuk, A. Andrushchak</i>   |

## FINAL SESSION

| Monday, November 13<br>9 <sup>00</sup> -11 <sup>00</sup> |
|--|
|--|

1. Concluding reports of Section Chairman.
2. Conference summary and closing.

## SPONSORS



**This conference has received funding from the European Union's Horizon 2020 research and innovation programme under the Marie Skłodowska-Curie grant agreement No 778156**



**Project "MAGE" – Innovative Optical/Quasioptical Technologies and Nano Engineering of Anisotropic Materials for Creating Active Cells with Substantially Improved Energy Efficiency**

## UNDER THE AUSPICES OF



**MINISTRY OF EDUCATION AND  
SCIENCE OF UKRAINE**



**LVIV POLYTECHNIC  
NATIONAL UNIVERSITY**

## **BOOK OF ABSTRACTS**



## CONTENT

### SECTION 1. INNOVATIVE MATERIALS

|  |            |
|--|------------|
| <b>Formation of the Nanocrystalline Phase of Active Dielectrics on the Surface and in the Pores of Synthetic Opals</b> | <b>1-1</b> |
| <i>V. Moiseienko, M. Derhachov, B. Abu Sal</i>   |            |
| <b>Silver-doped Lithium Triborate Glass for OSL Dosimetry</b>  | <b>1-2</b> |
| <i>V. Adamiv, Ya. Burak, N. Volod'ko, U. Dutchak, T. Izo, I. Teslyuk, A. Luchechko</i>                                 |            |
| <b>Quantum Computing of Physical Properties of Quantum Systems</b>   | <b>1-3</b> |
| <i>H. Laba, V. Tkachuk</i>   |            |
| <b>Raman Spectroscopy and Symmetry Analysis in Structure Determining of Nanoconfined Nanocrystals</b>                  | <b>1-4</b> |
| <i>Ya. Shchur, A.V. Kityk, V. Adamiv, I. Teslyuk, S. Vitusevich, A. Andrushchak</i>                                    |            |
| <b>MXenes, Their Optical Properties and Interactions with Electromagnetic Waves</b>                                    | <b>1-5</b> |
| <i>Y. Gogotsi</i>  |            |
| <b>Mesoporous Silica and Alumina as Efficient Supports for Solid Catalysts of Aldol Condensation Reaction</b>          | <b>1-6</b> |
| <i>R. Nebesnyi, I. Demydov, S. Khalameida, V. Sydorchuk, V. Ivasiv</i>   |            |
| <b>The Optimal Geometries of Piezoelectric Effect in Trigonal Crystals</b>   | <b>1-7</b> |
| <i>O. Buryy, M. Kyryk, A. Andrushchak</i>  |            |

### SECTION 2. OPTICAL AND QUASIOPTICAL TECHNIQUES FOR MATERIALS CHARACTERIZATION

|   |            |
|---|------------|
| <b>Optical Properties of Thin Film and Bulk Materials in the Visible and Infrared Spectrum Ranges</b>   | <b>2-1</b> |
| <i>A. Danylov, D. Vynnyk, V. Haiduchok</i>  |            |
| <b>Features of Photoelastic Properties of Ordered-structure Langasite Group Crystals</b>                | <b>2-2</b> |
| <i>N. Demyanyshyn, B. Mytsyk, Yu. Maksishko, A. Erba, J. Maul, B. Olhovyk, O. Buryy, A. Andrushchak</i> |            |

|   |             |
|---|-------------|
| <b>Optical Properties Investigation of Nanoporous Al<sub>2</sub>O<sub>3</sub> Matrices with Embedded ADP and KB-5 Crystals</b>                      | <b>2-3</b>  |
| <i>N. Andrushchak, D. Vynnyk, V. Haiduchok, A. Nikolenko, V. Adamiv, V. Strelchuk, O. Syrotynsky, A. Andrushchak</i>                                |             |
| <b>Photoelasticity of Ammonium Fluoroberylate Crystals</b>  | <b>2-4</b>  |
| <i>V. Stadnyk, B. Mytsyk, N. Demyanyshyn, P. Shchepanskyi, Y. Kost</i>  |             |
| <b>In situ X-ray synchrotron diffraction as a tool for the study of structural and electronic instabilities of solids</b>                           | <b>2-5</b>  |
| <i>L. Vasylechko, O. Pekinchak, O. Pavlovska, V. Hreb, A. Senyshyn</i>  |             |
| <b>Topological Transition in Quasi 2D-crystals</b>  | <b>2-6</b>  |
| <i>B. Lukiyanets, D. Matulka</i>  |             |
| <b>Supersymmetry and Entangled States in Quantum Optics</b>   | <b>2-7</b>  |
| <i>H. Laba, V. Tkachuk</i>  |             |
| <b>Control of Second-Harmonic Generation via Phase-Matched induced by Magnetization in Iron Garnet Epitaxial Thin Films</b>                         | <b>2-8</b>  |
| <i>I. Syvorotka, D. Guichaoua, N. Syvorotka, R. Wielgosz, A. Andrushchak, S. Taboukhat, B. Sahraoui</i>   |             |
| <b>Generation of Acoustic Vortices and Acousto-Optic Interactions with Acoustic Vortex Beams</b>  | <b>2-9</b>  |
| <i>I. Martynyuk-Lototska, M. Kostyrko, D. Adamenko, I. Skab and R. Vlokh</i>  |             |
| <b>The Experimental Definition of Electro-optical Parameters in the LiTaO<sub>3</sub> Crystals. Analytical Representation of Spatial Anisotropy</b> | <b>2-10</b> |
| <i>B. Olkhovyk, Y. Lozynskyi, Z. Kohut</i>  |             |
| <b>Comparative Investigation of Nonlinear Optical Responses in Various Lanthanide Coordination Compounds</b>  | <b>2-11</b> |
| <i>H. El Karout, A.V. Kityk, R. Wielgosz, S. Taboukhat, D. Guichaoua, A. Andrushchak, O. Krupka and B. Sahraoui</i>                                 |             |
| <b>Computer Simulation Studies of Collective Dynamics in Complex Metallic Glasses and Ionic Melts</b>   | <b>2-12</b> |
| <i>T. Bryk</i>  |             |
| <b>Vector Phase Matching in Orthorhombic Biaxial Crystals by Extreme Surface Method</b>   | <b>2-13</b> |
| <i>D. Shulha, O. Buryy, A. Andrushchak</i>  |             |

### SECTION 3. NANOENGINEERING TECHNOLOGIES AND PROCESSES

- Preparation of  $\text{Bi}_{12}\text{GeO}_{20}$  Nanocrystalline Structures** 3-1  
*Ya. Shchur, V. Adamiv, I. Teslyuk, A. Andrushchak*
- Structures of InSb for Infrared Photodiodes Obtained by the Method of Pulsed Cooling of a Saturated Solution-Melt** 3-2  
*M. Vakiv, S. Krukovskiy, I. Iznin, J. Kost, V. Arikov, O. Kulbachynskiy, O. Gudymienko, O. Dubikovskiy*
- Study of Coloumb Correlation Influence on SPPs Frequency Spectrum in Dielectric/Metal/Dielectric Structures** 3-3  
*P. Kostrobii, V. Polovyi, O. Pits*
- Multi-qubit Quantum Graph States and Studies of their Properties with Quantum Programming** 3-4  
*Kh. Gnatenko*
- Modeling the Separation Surface Influence on the Lattice Structure in Nanosystems** 3-5  
*P. Kostrobij, I. Ryzha, M. Sheremeta*
- Functionalised Selected Conjugated Compounds for Nonlinear Optical Applications** 3-6  
*B. Sahraoui, H. Karout, A, A.V. Kityk, Y. Shchur, A. Andrushchak, R. Wielgosz, O. Kityk, M. Lelonek, P. Göring, O. Krupka*
- Silica-Benzil and Alumina-Benzil Crystalline Nanocomposites: Textural Morphology and Nonlinear Optical Characterization** 3-7  
*A.V. Kityk, H. El Karout, B. Sahraoui, Y. Shchur, A. Andrushchak, R. Wielgosz, O. Kityk, J. Jędryka, Y. Slyvka, M. Lelonek, P. Göring, P. Huber*
- Effect of Photogeneration on Concentration of Excess Carriers in Si and Ge Crystals** 3-8  
*A. Danylov, B. Venhryn, S. Luniov, A. Korolyshyn, I. Senko, D. Afanassyev, A. Ratych, A. Andrushchak*

### SECTION 4. APPLICATIONS OF INNOVATIVE MATERIALS

- Development of sub-THz Modulators. Experience and Results** 4-1  
*Y. Yashchyshyn, V. Hajduchok, S. Krukowski, P. Bajurko, J. Sobolewski*

|  |            |
|--|------------|
| <b>Polymer-Containing Composites for Li<sup>+</sup> Intercalation Current Generation</b>   | <b>4-2</b> |
| <i>O. Balaban, N. Mitina, A. Zaichenko, O. Izhyk</i>   |            |
| <b>Femtosecond Laser-Induced Periodic Surface Structures: Theory and Applications</b>  | <b>4-3</b> |
| <i>I. Gnilityskyi</i>  |            |
| <b>Comparison of Series and Shunt GaN RF Switches for Millimeter-Wave Applications</b>   | <b>4-4</b> |
| <i>P. Bajurko, J. Sobolewski, Y. Yashchyshyn</i>   |            |
| <b>Why a Phosphor of the High Effective Atomic Number can be Useful for Dosimetry</b>  | <b>4-5</b> |
| <i>S. Ubizskii, O. Poshyvak, Ya. Zhydachevskyy</i>   |            |
| <b>Mercury Detection Sensor Based on the Structure of Amorphous Se Film/Au Nanoparticles</b>   | <b>4-6</b> |
| <i>M. Trunov, V. Rubish, V. Kyrylenko, M. Durkot</i>   |            |
| <b>Study of Relationship Between Nonlinear Optical Phenomena and the Molecular Structure of Specific Industrial Organic Compound</b> | <b>4-7</b> |
| <i>A. Aamoum, S. Taboukhat, A. Andrushchak, R. Wielgosz, M. Lelonek, P. Göring and B. Sahraoui</i>                                   |            |
| <b>Selenium Thin Films Application in THz Range</b>  | <b>4-8</b> |
| <i>A. Bendak, I. Senko, D. Vynnyk, V. Rubish</i>   |            |

## **Section 1**

# **INNOVATIVE MATERIALS**





# Formation of the Nanocrystalline Phase of Active Dielectrics on the Surface and in the Pores of Synthetic Opals

V. Moiseienko<sup>1</sup>, M. Derhachov<sup>1\*</sup>, B. Abu Sal<sup>2</sup>

<sup>1</sup>Oles Honchar Dnipro National University, Haharina Ave. 72, 49010 Dnipro, Ukraine

<sup>2</sup>Tafila Technical University, P.O. Box 40, Al-Eis 66141, Tafila, Jordan

\*Tel: (38056) 374 9822, Fax: (38056) 374 9841, e-mail: [derhachov.mp@gmail.com](mailto:derhachov.mp@gmail.com)

One of the modern trends in solid-state physics is the increasing interest in the properties of low-dimensional objects in which one, two, or three dimensions are confined on the nanometer scale. Spatial confinement significantly affects the electronic and vibrational spectrum and leads to the dominant impact of the nanocrystal surface on its properties. To date, several methods have been developed to produce nanocrystalline dielectrics with impurities of rare-earth and transition metal ions: sol-gel technology [1], laser ablation [2], organometallic reactions, precipitation of crystallites in glass [3].

This work concerns the melt- and solution-based technologies for growing nanocrystals of complex oxides on the surface and in the pores of synthetic opals. The nanostructured surface of submicron and nanometer spherical silica particles, which have an internal hierarchical structure of fractal type, acts as crystallization centers in this case. Bulk samples of nanocomposites fabricated by impregnating original opals with the melts of  $\text{Bi}_{12}\text{Si}(\text{Ge})\text{O}_{20}$ ,  $\text{Bi}_2\text{TeO}_5$ ,  $\text{NaBi}(\text{MoO}_4)_2$ ,  $\text{TeO}_2$ ,  $\text{Pb}_3(\text{P}_{0.5}\text{V}_{0.5}\text{O}_4)_2$ ,  $\text{Pb}_5\text{Ge}_3\text{O}_{11}$ ,  $\text{LiB}_3\text{O}_5$ ,  $\text{Li}_2\text{B}_4\text{O}_7$  as well as with the water solutions of  $\text{Ba}(\text{NO}_3)_2$ ,  $\text{LiIO}_3$ ,  $\text{KH}_2\text{PO}_4$  were characterized by SEM, XRD, optical and Raman spectroscopy techniques.

It was found that the melts of nonlinear dielectrics  $\text{Pb}_5\text{Ge}_3\text{O}_{11}$  and  $\text{LiB}_3\text{O}_5$  poorly wet the opal surface and practically did not enter the pores located in the opal volume. When the opals were soaked with  $\text{Li}_2\text{B}_4\text{O}_7$  melt, the temporal evolution of the composite content was observed. For the shortest soaking time (0.5 min), a low-frequency shift of the broadened Raman bands of  $\text{Li}_2\text{B}_4\text{O}_7$  was detected, while for the longer times the measured spectrum was identical to that of  $\alpha$ -quartz.

For  $\text{TeO}_2$ , a rare crystalline modification,  $\gamma$ - $\text{TeO}_2$ , non-formed under usual conditions, was revealed. Upon embedding of  $\text{Bi}_{12}\text{SiO}_{20}$ ,  $\text{Bi}_{12}\text{GeO}_{20}$  or  $\text{Bi}_2\text{TeO}_5$ , nanocrystalline phase of  $\text{Bi}_4\text{Si}_3\text{O}_{12}$  was observed on the surface and in the volume of original opal, together with one of the quartz polymorphs (cristobalite or tridymite, depending on the filler) in the opal volume.

No stoichiometry deviations and new phases were detected in  $\text{NaBi}(\text{MoO}_4)_2/\text{opal}$ ,  $\text{Pb}_3(\text{P}_{0.5}\text{V}_{0.5}\text{O}_4)_2/\text{opal}$  composites as well as in all composites fabricated by using the solution-based impregnation technique.

Average linear size of nanocrystals formed on the surface and in the volume of opal is in the range of 30 nm – 50 nm. Relative changes in lattice parameters of nanocrystals are no more than 0.1 % compared to those for corresponding single crystals.

The observed features of formation of nanocrystalline phase can be explained by interaction of the broken Si–O bonds on the silica particle surface with cations of the embedded substance. This interaction can result in releasing  $[\text{SiO}_4]$  tetrahedra from the chain inside the particle and involving them in formation of new crystal lattice when cooling. Besides, the concentration of cations and their charge state should be also considered. The mechanism of the  $\alpha$ -quartz phase formation in opal soaked with the  $\text{Li}_2\text{B}_4\text{O}_7$  melt is rather due to the local melting of silica particle's surface due to lithium-oxygen exothermic reaction.

[1] R.I. Zakharchenya (1995) *J. Sol-Gel Sci. Technol.* 6, 179-186.

[2] D.K. Williams et al. (1998) *J. Phys. Chem. B.* 102, 916-920.

[3] M.J. Dejneka (1998) *J. Non-Cryst. Sol.* 239, 149-155.



# Silver-doped Lithium Triborate Glass for OSL Dosimetry

V. Adamiv<sup>1,\*</sup>, Ya. Burak<sup>1</sup>, N. Volod'ko<sup>2,3</sup>, U. Dutchak<sup>3</sup>,  
T. Izo<sup>3</sup>, I. Teslyuk<sup>1</sup>, A. Luczechko<sup>4</sup>

<sup>1</sup>*O.G. Vlokh Institute of Physical Optics, 23 Dragomanov St., Lviv, 79005, Ukraine*

<sup>2</sup>*Department of Oncology and Radiology, Faculty of Postgraduate Education, Danylo Halitsky Lviv National Medical University, 69 Pekarska St., Lviv, 79010, Ukraine*

<sup>3</sup>*Department of radiation therapy, Lviv Oncology Regional Medical and Diagnostic Center, 2a Yaroslav Hashek St., Lviv, 79058*

<sup>4</sup>*Faculty of Electronics and computer technologies, Ivan Franko National University, 50 Drahomanov St., Lviv, 79005, Ukraine*

\*Tel: (380-32) 261 1488, e-mail: [adamiv@ifp.lviv.ua](mailto:adamiv@ifp.lviv.ua)

Over the past decades, solid-state dosimeters based on optically stimulated luminescence (OSL), in particular, on Ag<sup>+</sup>-activated phosphate glass, have become popular. However, the search for new and improved versions of the known working bodies for thermoluminescent (TL) and OSL dosimeters with better characteristics - sensitivity, moisture resistance, number of operating cycles, and cheaper prices - is still relevant.

Lithium triborate (LiB<sub>3</sub>O<sub>5</sub>) is one of the most well-known lithium borates due to the unique nonlinear optical properties of its single crystals. These crystals have interesting luminescent properties, in particular, photo- and thermoluminescence (PL and TL), which can be used for dosimetry [1]. However, LiB<sub>3</sub>O<sub>5</sub> single crystals have no prospects for use in dosimetry because of the high cost and complexity of doping. The use of glass of a similar composition simplifies and reduces the cost of obtaining samples, in particular because the high content of boron oxide (B<sub>2</sub>O<sub>3</sub>) in the charge facilitates the formation of glass due to the high tendency of B<sub>2</sub>O<sub>3</sub> to glass transition. Another argument in favor of borate glasses is that they allow for the formation of pyroceramics, or crystallized glass. This was confirmed experimentally for LiB<sub>3</sub>O<sub>5</sub>:Ag-doped glass [2].

Our work [2,3] on the study of the thermoluminescent properties of LiB<sub>3</sub>O<sub>5</sub> and LiB<sub>3</sub>O<sub>5</sub>:Ag glasses made it possible to conclude that LiB<sub>3</sub>O<sub>5</sub>:Ag can be effectively used in dosimetry and, in the future, that LiB<sub>3</sub>O<sub>5</sub>:Ag samples can be used for dosimeters based on OSL.

The samples were irradiated with γ-rays under real conditions of radiation therapy using the remote γ-therapy apparatus "TERAGAM" Co(60) at the Lviv Regional Cancer Treatment and Diagnostic Center. The results of the analysis of the OSL spectra of LiB<sub>3</sub>O<sub>5</sub>:Ag glass under 220 nm light excitation on samples irradiated with doses of 1.5 and 3 Gy and unirradiated samples showed high sensitivity of our material and a clear dependence on the received radiation dose.

The increased sensitivity of LiB<sub>3</sub>O<sub>5</sub> to neutrons due to the presence of lithium isotopes Li(6) and boron B(10) with large cross sections of interaction with thermal neutrons σ (945 and 3840 barns, respectively) allows us to manufacture OSL and TL dosimeters for almost the entire spectrum of radiation exposure, including neutrons. And this is very important for medicine, since neutrons (neutron therapy) are used in the treatment of human body organs damaged by cancer in addition to traditional gamma quanta and high-energy electrons [4].

[1] I.N. Ogorodnikov, et al. (2001) *Rad. Meas.* 33, 577-581.

[2] V.T. Adamiv et al. (2019) *Ukr. J. Phys. Opt.*, 20, 159-167.

[3] V.T. Adamiv et al. (2018) *IEEE 8th ICNAP, Ukraine, (Proceeding)* 2, 1-5.

[4] J.M. Gómez-Ros, R. Bedogni, C. Domingo, (2023) *Radiat. Meas.* 161, 106908.



# Quantum Computing of Physical Properties of Quantum Systems

H. Laba<sup>1</sup>, V. Tkachuk<sup>2\*</sup>

<sup>1</sup>*Department of Applied Physics and Nanomaterials Science, Lviv Polytechnic National University*

<sup>2</sup>*Department for Theoretical Physics, Ivan Franko National University of Lviv*

\*e-mail: [voltkachuk@gmail.com](mailto:voltkachuk@gmail.com)

Recently there was made great efforts in developing quantum algorithms for noisy intermediate-scale quantum computers. For the calculation of the energy spectrum of a quantum system there was proposed the quantum algorithm which is stable concerning the noise of present quantum computers.

The main problem for studying the thermodynamic properties of a quantum system and calculating partition function is the simulation on a quantum computer of the Boltzmann factor that is not a unitary operator. Quantum computers deal with unitary operations and it is possible in principle to generate arbitrary unitary operators (operators of the evolution of the quantum system) using quantum gates. We realize the Boltzmann factor of the Ising model on a quantum computer as a trace of some evolution operator with effective Hamiltonian over ancilla spins (qubits). As a result of the relation of the operator of evolution with the Boltzmann factor, we find the partition function of the Ising model on a quantum computer. The realization of the Boltzmann factor on quantum computers allows also us to find the ground state of a quantum system, in particular for the Ising model.

As an example, the partition function of the Ising model for two-spin cluster is calculated on IBM's quantum computer. The possibility of finding ground state is also demonstrated for two-spin cluster. The results obtained on quantum computer are in good agreement with theoretical ones.



# Raman Spectroscopy and Symmetry Analysis in Structure Determining of Nanoconfined Nanocrystals

Ya. Shchur<sup>1\*</sup>, A.V. Kityk<sup>2</sup>, V. Adamiv<sup>3</sup>, I. Teslyuk<sup>3</sup>, S. Vitusevich<sup>4</sup>,  
A. Andrushchak<sup>5</sup>

<sup>1</sup>*Institute for Condensed Matter Physics, Svientsitskii 1, 79011, Lviv, Ukraine*

<sup>2</sup>*Faculty of the Electrical Engineering, Czestochowa University of Technology, Al. Armii Krajowej 17, 42-200 Czestochowa, Poland*

<sup>3</sup>*O.G. Vlokh Institute of Physical Optics, Dragomanov str. 23, 79005, Lviv, Ukraine*

<sup>4</sup>*Institute of Bioelectronics (IBI-3), Forschungszentrum Juelich, D-52425 Juelich, Germany*

<sup>5</sup>*Lviv Polytechnic National University, Bandera str. 12, 79013, Lviv, Ukraine*

\*e-mail: [shchur@icmp.lviv.ua](mailto:shchur@icmp.lviv.ua)

We report the general principles used for crystal structure determining of nanosized crystals embedded to porous matrices of SiO<sub>2</sub>. The use of polarized Raman spectroscopy combined with the rigorous group theory analysis of lattice dynamics can reveal the structural features of many crystals. Beside of group-theory we use the first-principles calculations of lattice dynamics which allow the immediate numerical interpreting of all spectroscopic data. The route of this technique is demonstrated by using the examples of KH<sub>2</sub>PO<sub>4</sub> and Ba(NO<sub>3</sub>)<sub>2</sub> crystals.

In KH<sub>2</sub>PO<sub>4</sub> crystal, we performed the scrupulous symmetry analysis of four vibrational ranges corresponded to (1, below ~300 cm<sup>-1</sup>) external lattice vibrations, (2, 300-600 cm<sup>-1</sup>) internal bending PO<sub>4</sub> group modes, (3, 900-1100 cm<sup>-1</sup>) internal stretching PO<sub>4</sub> group modes and (4, >1200 cm<sup>-1</sup>) proton modes. The experimental data detected on these spectral ranges were carefully checked both in bulk single crystal and that of KH<sub>2</sub>PO<sub>4</sub>&SiO<sub>2</sub> nanocomposite. After subtracting the Raman response of SiO<sub>2</sub> matrix, it appears that the Raman spectrum of KH<sub>2</sub>PO<sub>4</sub>&SiO<sub>2</sub> composite resembles in main spectral features the Raman spectrum of KH<sub>2</sub>PO<sub>4</sub> single crystal. In other words, detailed spectral analysis proves the crystallization of KH<sub>2</sub>PO<sub>4</sub> nanocrystals inside the pores of SiO<sub>2</sub> matrix.

The similar symmetry analysis was applied to Ba(NO<sub>3</sub>)<sub>2</sub> crystal, where the vibrational range may also be divided into four subregions, i.e. (1, below ~200 cm<sup>-1</sup>), (2, 700-800 cm<sup>-1</sup>), (3, ~1600 cm<sup>-1</sup>) and (> 1360 cm<sup>-1</sup>). However, to separate the normal modes transformed according to A<sub>g</sub> and E<sub>g</sub> symmetries a special spectroscopic polarizer technique was used. Analyzing both the Raman line intensities and their full widths at half maximums (FWHM) we have established the spatial nanoconfinement impact onto the crystal structure of nanosized Ba(NO<sub>3</sub>)<sub>2</sub> crystals embedded to pores of SiO<sub>2</sub> matrix. We have also proved an existence of the large ~10-20 μm single crystal regions in a network of pores with a diameter of ~10-12 nm.

**Acknowledgment:** This work has received funding from the National Research Foundation of Ukraine (Project 2021.01/0410) and from the European Union's Horizon 2020 research and innovation programme under the Marie Skłodowska-Curie grant agreement No.778156.



# MXenes, Their Optical Properties and Interactions with Electromagnetic Waves

Y. Gogotsi<sup>1,2\*</sup>

<sup>1</sup>A.J. Drexel Nanomaterials Institute and Department of Materials Science and Engineering, Drexel University, Philadelphia, PA 19104, USA

<sup>2</sup>Sumy State University, Department of Nanoelectronics, Sumy, Ukraine

\*e-mail: [gogotsi@drexel.edu](mailto:gogotsi@drexel.edu)

MXenes (carbides and nitrides of early transition metals) are a very large family of 2D materials. They have a chemical formula of  $M_{n+1}X_nT_x$ , where M represents a transition metal (Ti, Mo, Nb, V, Cr, etc.), X is either carbon and/or nitrogen ( $n=1, 2, 3$  or  $4$ ), and  $T_x$  represents surface terminations. The diversity in compositions ( $>50$  MXenes have already been reported,  $>100$  stoichiometric structures predicted), availability of solid solutions on M and X sites, and control of surface terminations, such as O, OH, F, Cl, S, etc., offer a plethora of structures and chemistries to investigate [1]. Combining the plasmonic and non-linear optical properties with ease in processing, high electronic conductivity (over 20,000 S/cm) and mechanical strength, which exceed other solution-processable 2D materials, MXenes have the characteristics necessary to develop as optical and electronic materials [2]. Inherent to their 2D structure, the charge carriers responsible for MXene's optical responses and electronic transport are very close to an external interface that has exceptional ability to undergo reversible chemical and electrochemical reactions to add or change surface terminations. By design of the MXene composition, the carrier plasma can be rendered either sensitive to or uncommonly robust against the resulting changes in band structure and state-filling. MXenes offer chemically controlled optical and electronic properties that facilitate new ways of influencing material interactions with electromagnetic waves over UV-vis, IR, THz, and even GHz ranges [2-4]. MXenes have already shown great promise in applications such as electromagnetic interference shielding, antennas, thermal radiation management, etc. In this talk, I show that the optical, electronic and transport properties of MXenes can be controlled by tuning their chemical composition. This presentation will also demonstrate electrochemical modulation of the optoelectronic properties [4] and describe potential applications of MXenes in photonic and optoelectronic devices, such as electron transport layers for solar cells, optical sensors, electrochromic devices, metamaterials, EMI shields, etc [1,3].

[1] A. Vahid Mohammadi, J. Rosen, Y. Gogotsi (2021) *Science*, 372, eabf1581.

[2] K. Maleski, C. E. Shuck, A. Fafarman, Y. Gogotsi (2020) *Advanced Optical Materials*, **9** (4) 2001563.

[3] M. Han, D. Zhang, A. Singh, T. Hryhorchuk, C. E. Shuck, T. Zhang, L. Bi, B. McBride, V. B. Shenoy, Y. Gogotsi (2023), *Materials Today*, **45**, 31-39.

[4] M. Han, D. Zhang, C. E. Shuck, B. McBride, T. Zhang, R. (John) Wang, K. Shevchuk, Y. Gogotsi, (2023), *Nature Nanotechnology*, (2023) **18** (4), 373–379.



# Mesoporous Silica and Alumina as Efficient Supports for Solid Catalysts of Aldol Condensation Reaction

R. Nebesnyi<sup>1\*</sup>, I. Demydov<sup>1</sup>, S. Khalameida<sup>2</sup>, V. Sydoruk<sup>2</sup>, V. Ivasiv<sup>1</sup>

<sup>1</sup>Lviv Polytechnic National University, 12 S. Bandery, 79013 Lviv, Ukraine

<sup>2</sup>Institute for Sorption and Problems of Endoecology, 13 Naumov St., 03164 Kyiv, Ukraine

\*Tel: (38032) 258 2413, e-mail: [roman.v.nebesnyi@lpnu.ua](mailto:roman.v.nebesnyi@lpnu.ua)

Nanoporous silica and alumina have extremely wide application in various fields of chemistry and physics. Here we report the use of mesoporous silica and alumina as efficient supports for solid catalysts of aldol condensation reactions, in particular for the catalysts of acrylic acid (AA) synthesis via aldol condensation reaction of acetic acid with formaldehyde.

The support plays huge role in heterogeneous catalysis and has a direct effect on the structural and morphological characteristics of catalysts. In addition, the support's nature, despite its chemical inertness, affects the chemical reaction. Previously we reported good results using  $\text{Al}_2\text{O}_3$  as supports for B-P-V-W- $\text{O}_x$  catalysts (AA yield per pass 57.2%, AA selectivity 89.0%) and  $\text{SiO}_2$  supports (AA yield per pass 43.7%, AA selectivity 84.9%) [1].

It was established that the pore size and specific surface area of the catalyst, which can be effectively controlled by hydrothermal treatment of the catalyst support, affect the activity and selectivity of the catalyst [2]. At the same time, the best AA selectivity and yield are reached on the catalyst with the pore size of at least 12 nm, specific surface area 193  $\text{m}^2/\text{g}$ , and pore volume 0.72  $\text{ml/g}$  (90.5% and 67.6%, respectively). Further studies confirmed such approach and the catalyst based on fumed silica (Fig. 1) with an average pore size 32 nm, specific surface area 126  $\text{m}^2/\text{g}$  with pore volume 1.08  $\text{ml/g}$  allowed to synthesize AA with 68.8% yield at 94.1% selectivity. Based on this data, it was concluded that significant free pore volume is of great importance for the free transport of reagents and the condensation reaction products, reducing the selectivity of by-products formation (subsequent condensation) in the reaction zone and slowing down the coking of catalysts.

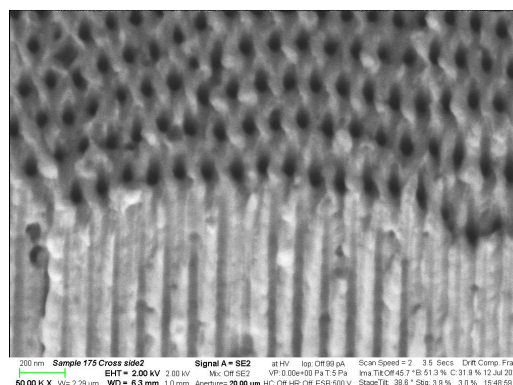
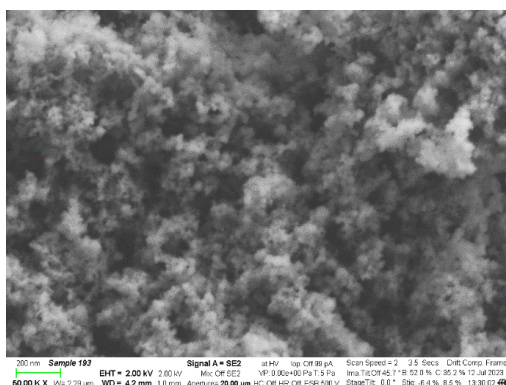


Figure 1. TEM image of B-P-V-W- $\text{O}_x/\text{SiO}_2$  catalyst Figure 2. TEM image of  $\text{SiO}_2$  structured support.

The significant dependence of the parameters of the condensation process on the catalyst's porous structure makes it reasonable to study aldol condensation reactions on catalysts with structured supports [3]. From this point of view, the use of novel structured mesoporous  $\text{Al}_2\text{O}_3$  and  $\text{SiO}_2$  is very promising (Fig. 2). Further improvement in selectivity control allows to simplify the product separation scheme, which is important for the prospects of industrial implementation of the gas-phase catalytic synthesis of AA by aldol condensation reaction.

[1] R. Nebesnyi, V. Sydoruk, V. Ivasiv et al., *Theor. And Exp. Chem.* 56(4) (2020) 268-274.

[2] R. Nebesnyi, Z. Pikh, V. Sydoruk et al., *Applied Catalysis A, General* 594 (2020) 117472.

[3] M. Arumugam, O. Kikhtyanin, A. Osatiashtiani et al., *Sustainable Energy&Fuels*. 7 (2023) 3047.

**"Innovative Materials and NanoEngineering" (IMNE'2023)**

**November 10-13, 2023, Dovgoluka, Ukraine**



# The Optimal Geometries of Piezoelectric Effect in Trigonal Crystals

O. Buryy<sup>1\*</sup>, M. Kyryk<sup>1</sup>, A. Andrushchak<sup>1</sup>

<sup>1</sup> Lviv Polytechnic National University, 12 Stepana Bandery str., 79013 Lviv, Ukraine

\* Tel: (0322) 258 2696, e-mail: [oleh.a.buryi@pnu.ua](mailto:oleh.a.buryi@pnu.ua)

Piezoelectric materials have traditionally attracted considerable attention due to their ability to convert mechanical energy into electrical one and vice versa. This property makes them suitable for a variety of applications such as sensors, actuators, transducers, generators of acoustic waves etc. As it follows from the theoretical analysis of the piezoelectric effect, its magnitude depends significantly on the character of the applied mechanical stress field. At that an important parameter that characterizes the energy efficiency of piezoelectric device is the electromechanical coupling coefficient (ECC) which is a numerical measure of the conversion efficiency between electrical and mechanical energy. The ECC is determined as the square root of the ratio of electrical energy to the sum of electrical and elastic ones, and can be calculated in accordance with the expression

$$K = \frac{E_i d_{ijk} \sigma_{jk}}{\sqrt{(E_i \varepsilon_{ij} E_j) (\sigma_{ij} s_{ijkl} \sigma_{kl})}}, \quad (1)$$

where  $E_i$  are the components of electrical field intensity,  $\sigma_{jk}$  are the components of mechanical stress,  $d_{ijk}$  are piezoelectric coefficients,  $\varepsilon_{ij}$  are the dielectric permittivities,  $s_{ijkl}$  are the elastic compliance coefficients, over repeating indices the summation is carried out in (1).

To ensure the the highest possible value of the ECC, the optimal cut of piezoelectric crystal should be determined. As it is followed from (1), the ECC depends on the direction of the electrical field and the the relationship between the components of the mechanical stress tensor, but not on the absolute values of the electrical intensity or the mechanical stress. Thus, the determination of the optimal geometry of piezoelectric effect can be carried out in the same way as for the cases of optically induced or non-linear optical effects, i.e. by construction and analysis of the extreme surfaces representing the possible maxima of piezoelectric effect for all possible directions of electrical field. Here such a problem is considered for trigonal crystals belonging to point groups of symmetry 3m and 32 - lithium niobate and tantalate (3m), langasite and quartz (32).

The problem is analyzed in two formulations: (i) the uniaxial pressure is applied; (ii) the mechanical stress field has got the arbitrary character, i.e. six independent components  $\sigma_{jk}$  are considered as the parameters of optimization (the general case). As it is shown, in the case of uniaxial pressure the optimal geometry of the effect is significantly different from orthogonal one for crystals of point group 3m (LiNbO<sub>3</sub>, LiTaO<sub>3</sub>), whereas for crystals of point group 32 (La<sub>3</sub>Ga<sub>5</sub>SiO<sub>14</sub>, SiO<sub>2</sub>), on the contrary, it is practically coincides with orthogonal, while the directions of electric tension and uniaxial compression are mutually perpendicular. The highest value of the EEC was found for the lithium niobate crystal, it is equal to 0.87, whereas for LiTaO<sub>3</sub>  $K = 0.47$ , for La<sub>3</sub>Ga<sub>5</sub>SiO<sub>14</sub>  $K = 0.17$ , for SiO<sub>2</sub>  $K = 0.12$ . In the general case, the highest achievable values of the EEC increase in comparison with the case of uniaxial pressure within units - tens of percent: 7% for LiNbO<sub>3</sub> (till 0.93), 33% for SiO<sub>2</sub> (till 0.16). The obtained results can be used to increase the efficiency of piezoelectric devices.

**Acknowledgments:** These results are part of a project that has received funding from the EU Horizon 2020 research and innovation programme under the Marie Skłodowska-Curie grant agreement No 778156. This work was also supported by the Ministry of Education and Science of Ukraine in the frame of project 'Nanoelectronics' (0123U101695).



**Section 2**

**OPTICAL AND QUASIOPTICAL TECHNIQUES FOR  
MATERIALS CHARACTERIZATION**





# Optical Properties of Thin Film and Bulk Materials in the Visible and Infrared Spectrum Ranges

A. Danylov<sup>1\*</sup>, D. Vynnyk<sup>1</sup>, V. Haiduchok<sup>2</sup>

<sup>1</sup>Lviv Polytechnic National University, 12, S. Bandera St., 79013 Lviv, Ukraine

<sup>2</sup>Scientific Research Company "Carat", 202, Stryyska St., 79031 Lviv, Ukraine

\*e-mail: [andriy.b.danylov@lpnu.ua](mailto:andriy.b.danylov@lpnu.ua)

The terahertz band is becoming an increasingly attractive research area due to a number of applications in telecommunications, medicine, security, and more [1]. Promising materials in the terahertz range include materials with low or high absorption in a certain region of the terahertz spectrum and low dispersion of optical constants in the region. Depending on the application, such materials have different requirements. In particular, when creating optical modulators and filters of the THz range, it is important to ensure a large modulation depth and a significant switching speed. Therefore, such materials should have a low concentration of carriers and their short lifetime. Due to the strong absorption of free carriers in the THz spectrum range, one of the ways to control THz-radiation in devices based on such materials is the optical excitation of free carriers by irradiating the material with light from a laser or a powerful lamp in the visible spectrum range. At the same time, it is important to pre-investigate the optical properties of materials in the visible-near-infrared region to establish whether the materials will be able to provide a sufficient level of carrier generation and at which spectrum frequencies.

By means of the two-beam spectrophotometer Shimadzu UV-3600, we measured transmission and reflection spectra in the 200-3000 nm spectrum range for Se thin films deposited on quartz wafers, flat plates of silicon crystals with various resistance values (up to high resistive silicon), and BGO and BSO crystals, which are considered attractive for application in the terahertz band. Based on the transmission spectra of selenium films, the film thicknesses, absorption coefficients, and refraction indices were determined in the visible-IR spectrum range using the Swanepoel method [2] within the scope of the model of a homogeneous thin film on the surface of a transparent thick substrate. Absorption coefficients and refractive indices for silicon crystals, BGO and BSO were also determined according to the scheme proposed in [3]. Depending on the structure of material bands, the band gap was determined using the Tauc method [4] and the approach [5]. The obtained results were in good coincidence with the results of other researchers and reference data.

**Acknowledgements.** This work was supported by the National Research Foundation of Ukraine (project #2021.01/0410).

- [1] D. Saeedkia, Handbook of terahertz technology for imaging, sensing and communications (2013) Ed. Woodhead Publishing Limited, UK.
- [2] R. Swanepoel (1983) *J. Phys. E.* 16, 1214-1222.
- [3] J C Manificier, J Gasiot and J P Fillard (1976) *J. Phys. E: Sci. Instrum.* 9, 1002-1004.
- [4] J. Tauc, A. Menth (1972) *J. Non-Crystal Sol.* 8–10, 569-585.
- [5] M. Isik, S. Delice, N.M. Gasanly, et al (2020) *Ceram Int.* 46, 9, 12905-12910.



## Features of Photoelastical Properties of Ordered-structure Languasite Group Crystals

N. Demyanyshyn<sup>1\*</sup>, B. Mytsyk<sup>1</sup>, Yu. Maksishko<sup>1</sup>, A. Erba<sup>2</sup>, J. Maul<sup>2</sup>,  
B. Olhovyk<sup>3</sup>, O. Buryy<sup>3</sup>, A. Andrushchak<sup>3</sup>

<sup>1</sup>Karpenko Physico-Mechanical Institute, 5 Naukova St., Lviv, 79601, Ukraine

<sup>2</sup>Universita di Torino, Via Giuria 5, 10125 Torino, Italy

<sup>3</sup>Lviv Polytechnic National University, 12 Bandery St., Lviv, 79013, Ukraine

\*Tel: (096) 664 85 06, e-mail: [nmdem@ukr.net](mailto:nmdem@ukr.net)

Experimental and theoretical studies of languasite group crystals (LGS) are driven by their unique physical properties. These crystals are characterized by high-temperature stability of elastic and piezoelectric coefficients, low acoustic wave attenuation, especially at high frequencies, substantial piezoelectric effect, and a high electromechanical coupling coefficient [1-4]. Recent investigations of photoelastical effects, including piezooptical (POE), elastooptical (EIOE), and acoustooptical (AO) effects in crystals of this group, demonstrate their potential using as sensitive elements in electromagnetic radiation modulators [5-7].

In this work, for ordered-structure LGS crystals, experimental methods (interferometry and polarization optics) and theoretical methods (quantum-mechanical calculations and construction of indicative surfaces) were employed to determine matrices of absolute piezo- and elastooptical coefficients (POC and EIOC, respectively). The dispersion of POC and EIOC, as well as the anisotropy of POE and EIOE, were investigated.

Based on quantum-mechanical calculations of POC and EIOC, regularities in the variations of photoelastical properties of CTGS, CNGS, BTGS, and CNAS crystals were revealed, linked to changes in elemental composition. It was established that:

- a) Increasing the unit cell volume of the crystal lattice enhances the magnitude of the piezooptical effect in languasite group crystals;
- b) The dominance of longitudinal or transverse POE or EIOE (in terms of their magnitude) is associated with the ratio of lattice parameters  $c/a$ : the smaller this ratio, the greater the transverse POE or EOE effect.
- c) The substitution of  $Ga^{3+}$  ions in the structure of calcium halogen-manates with  $Al^{3+}$  ions were found to be effective. This not only reduces the cost of the corresponding material but also improves its elastooptical properties.

**Acknowledgment:** This work has received funding from the National Research Foundation of Ukraine (Project 2020.02/0211) and from the European Union's Horizon 2020 research and innovation programme under the Marie Skłodowska-Curie grant agreement No. 778156.

- [1] Fu X., Villora E., Matsushita Y., Kitanaka Y., Noguchi Y., Miyayama M., Shimamura K., Ohashi N. (2016) *J. Ceramic Soc. Jap.* 124, 523-527.
- [2] Kaminskii A., Belokoneva E., Mill B., Pisarevskii Yu., Sarkisov S., Silvestrova I., Butashin A., Khodzhabyan G. (1984) *Phys. Stat. Sol.(a)*. 86, 345-362.
- [3] Andreev I., Dubovik M. (1984) *Sov. Tech. Phys. Lett.* 10, 205-207.
- [4] Xin Y., Shaojun Z., Jiyang W. (2005) *J. Opt. Soc. of America B*. 22, 394-397.
- [5] Mytsyk B., Suhak Y., Demyanyshyn N., Buryy O., Syvorotka N., Sugak D., Ubizskii S., Fritze H. (2020) *Appl. Optics*. 59, 8951-8958.
- [6] Demyanyshyn N.M., Suhak Yu., Mytsyk B.G., Buryy O.A., Maksishko Yu.Ya., Sugak D., Fritze H. (2021) *Optical Materials*. 119, 111284.
- [7] Buryy O., Demyanyshyn N., Mytsyk B., Andrushchak A., Sugak D. (2022) *Optics Continuum*. 1, 1314-1323.



## Optical Properties Investigation of Nanoporous $\text{Al}_2\text{O}_3$ Matrices with Embedded ADP and KB-5 Crystals

N. Andrushchak<sup>1\*</sup>, D. Vynnyk<sup>1</sup>, V. Haiduchok<sup>2</sup>, A. Nikolenko<sup>3</sup>, V. Adamiv<sup>4</sup>,  
V. Strelchuk<sup>3</sup>, O. Syrotynsky<sup>5</sup>, A. Andrushchak<sup>1</sup>

<sup>1</sup> Lviv Polytechnic National University, 12 S. Bandery str., Lviv 79013, Ukraine.

<sup>2</sup> Scientific Research Company «Electron-Carat», 202 Stryyska str., Lviv 79031, Ukraine.

<sup>3</sup> V.E. Lashkaryov Institute of Semiconductor Physics, National Academy of Sciences of Ukraine, 41 Prosp. Nauky, 03028 Kyiv, Ukraine

<sup>4</sup> Department of Optical Materials, Vlokh Institute of Physical Optics, 23 M. Drahomanova str., Lviv 79005, Ukraine

<sup>5</sup> Private Enterprise Softpartners, 15 Smal-Stockogo str., Lviv 79029, Ukraine

\*e-mail: [nazariy.a.andrushchak@lpnu.ua](mailto:nazariy.a.andrushchak@lpnu.ua)

In works [1, 2], the optical properties of nanoporous  $\text{Al}_2\text{O}_3$  matrices produced by the German company Smartmembrans company with ADP, KDP, and KB-5 crystals introduced into the pores were investigated. It was established that nanoporous  $\text{Al}_2\text{O}_3$  matrices with ADP crystals introduced into the pores have a reflection coefficient of <1% in the spectral range of 1.0-10.0  $\mu\text{m}$ . It is shown that for these structures in the 1.0-3.0  $\mu\text{m}$  range of wavelengths, there is a diffuse scattering of ~80%. However, the reasons for such dispersion have not been established.

This problem was considered in this work, and it was established that the surface of these matrices has a decisive influence on the reflection of nanoporous  $\text{Al}_2\text{O}_3$  matrices with ADP crystals introduced into the pores. As a result of the conducted research, it was also established that the transmittance of both pure nanoporous  $\text{Al}_2\text{O}_3$  matrices and matrices with introduced ADP crystals is less than 1% in a wide spectral range. The range is 2.5-200  $\mu\text{m}$  for nanoporous  $\text{Al}_2\text{O}_3$  matrices with embedded ADP crystals and 5.0-200  $\mu\text{m}$  for pure nanoporous  $\text{Al}_2\text{O}_3$  matrices.

In the investigated samples with embedded KB-5 crystals, the measured optical transmission and reflection parameters differed from similar parameters from nanoporous matrices with embedded ADP crystals.

**Acknowledgment:** This work was supported by the National Research Foundation of Ukraine (project #2021.01/0410).

[1] N. Andrushchak et al. (2018) *2018 IEEE 8th International Conference Nanomaterials: Application & Properties (NAP)*, Zatoka, Ukraine, 2018, pp. 1-4.

[2] N. Andrushchak et al. (2022) *2022 IEEE 12th International Conference Nanomaterials: Applications & Properties (NAP)*, Krakow, Poland, 2022, pp. NCI02-1-NCI02-4.



# Photoelasticity of Ammonium Fluoroberylate Crystals

V. Stadnyk<sup>1</sup>, B. Mytsyk<sup>2\*</sup>, N. Demyanyshyn<sup>2</sup>, P. Shchepanskyi<sup>1</sup>, Y. Kost<sup>2</sup>

<sup>1</sup>Ivan Franko Lviv National University, 19 Dragomanova St., Lviv 79005, Ukraine

<sup>2</sup>Karpenko Physico-Mechanical Institute, 5 Naukova St., 79060 Lviv, Ukraine

Tel: +38(032) 2296 752, e-mail: [mytsyk@ipm.lviv.ua](mailto:mytsyk@ipm.lviv.ua)

Rhombic crystals of the  $A_2BX_4$  group, such as  $K_2ZnCl_4$ ,  $RbH_2AsO_4$ ,  $(NH_4)_2SO_4$ , etc., have large piezo- and elasto-optic coefficients [1], as well as high acousto-optic (AO) efficiency, which is 1-2 orders of magnitude higher than in known AO materials (quartz, strontium borate, langasite group), suitable for AO modulation of light in the ultraviolet region of the spectrum.

In this paper, all independent piezo-optic coefficients  $\pi_{im}$  of ammonium fluoroberylate  $(NH_4)_2BeF_4$  crystal are determined using the interferometric method. All independent elasto-optic coefficients  $p_{ik}$  are calculated on the basis of  $\pi_{im}$  and elastic stiffness coefficients  $C_{mk}$ . Great attention is paid to the reliability of the  $\pi_{im}$  values. For this, the maximum possible number of experimental geometries was used, both on direct-cut samples and on  $45^\circ$ -cut samples. Several  $\pi_{im}$  coefficients have atypically large values  $\sim (10-13) \cdot 10^{12} \text{ m}^2/\text{N}$ . An analysis of the spatial anisotropy of piezo- and elasto-optic effects was carried out on the basis of indicative surfaces and the maximum values of these effects were found, and their spherical coordinates were indicated. An example of indicative surface of ammonium fluoroberylate crystal is shown in Fig. 1. The coefficients of acousto-optic figure of merit  $M_2$  were determined for several geometries of acousto-optic interaction. The largest coefficients correspond to  $p_{23}$  and  $p_{33}$  coefficients and are  $12.2 \cdot 10^{15} \text{ s}^3/\text{kg}$  and  $10.7 \cdot 10^{15} \text{ s}^3/\text{kg}$ , respectively.

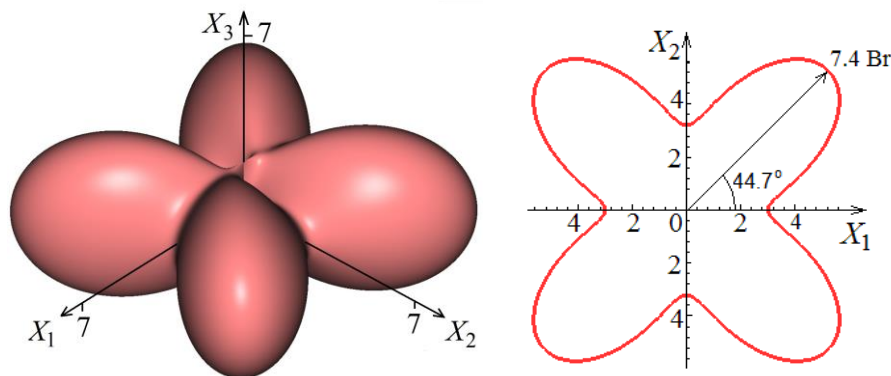


Fig. 1. Indicative surface of the transverse POE in ammonium fluoroberylate crystals and its intersections by the principal crystal-physics plane  $X_1$ ,  $X_2$ ; all in units  $10^{12} \text{ m}^2/\text{N}$ .

Based on the indicated  $M_2$  values, we can classify ammonium fluoroberylate among the best AO materials for the ultraviolet region of the spectrum, since in terms of these  $M_2$  coefficients the studied crystals significantly exceed the  $M_2$  of the model AO material of quartz, and the lower limit of  $(NH_4)_2BeF_4$  crystal transmission spectrum lies in the deep UV region  $\sim 250 \text{ nm}$ .

**Acknowledgment:** This work has received funding from the National Research Foundation of Ukraine (Project 2020.02/0211) and from the European Union's Horizon 2020 research and innovation programme under the Marie Skłodowska-Curie grant agreement No. 778156.

[1] Mytsyk B., Stadnyk V., Demyanyshyn N., Kost Ya., Shchepanskyi P. (2019) *Opt. Mat.* 88, 723-728.



## ***In situ* X-ray synchrotron diffraction as a tool for the study of structural and electronic instabilities of solids**

**L. Vasylechko<sup>1\*</sup>, O. Pekinchak<sup>1</sup>, O. Pavlovska<sup>1</sup>, V. Hreb<sup>1</sup>, A. Senyshyn<sup>2</sup>**

<sup>1</sup>*Lviv Polytechnic National University, 12 Bandera St., 79013 Lviv, Ukraine*

<sup>2</sup>*Forschungs-Neutronenequelle Heinz Maier-Leibnitz FRM-II, Technische Universität München, Lichtenbergstrasse 1, D-85748 Garching b. München, Germany.*

\* e-mail: [Leonid.O.Vasylechko@lpnu.ua](mailto:Leonid.O.Vasylechko@lpnu.ua)

In situ temperature-dependence powder diffraction examinations and analysis of thermal expansion is a very sensitive tool not only for the study of structural phase transformations, but also for the investigation of diverse electronic and magnetic phase transitions occurring in complex oxide and intermetallic systems. Here, we present the results of the comprehensive studies of the thermal behavior of several classes of materials obtained in our laboratory over the past two decades. The corresponding low- and high-temperature diffraction experiments were realized at the European synchrotron radiation sources ESRF (Grenoble), HASYLAB@DESY (Hamburg) and ALBA (Barcelona) thanks to our long-term cooperation with the International Centre of Diffraction Data (ICDD) in the frames of the Grant-in-Aid program.

It was revealed that several technologically important rare earth (RE) gallates and aluminates with a perovskite structure exhibit diverse anomalies in the lattice expansion, i.e. an abnormal sigmoidal temperature dependence of the unit cell dimensions in  $\text{YAlO}_3$  (YAP),  $\text{GdAlO}_3$  (GAP) and  $\text{NdGaO}_3$  (NGP), a negative thermal expansion in  $\text{PrGaO}_3$  below 120 K and the occurrence of LT isostructural phase transition in the NGP single crystal between RT and 100 K [1]. An unusual sequence of structural phase transitions was found in  $\text{CeAlO}_3$ , which undergoes a transformation from LT tetragonal to HT cubic structure through intermediate orthorhombic and rhombohedral perovskite structures. Among the mixed RE aluminates and gallates with orthorhombic perovskite structure, a unique phenomenon of the lattice parameter crossover with the appearance of metrically cubic structures has been discovered [1]. Pronounced anomalies in the lattice expansion were found in the mixed RE cobaltites  $\text{R}_{1-x}\text{R}'_x\text{CoO}_3$ , cobaltites-ferrites, cobaltites-chromites, and cobaltites-gallates  $\text{RCo}_{1-x}\text{M}_x\text{O}_3$  ( $\text{M} = \text{Fe, Cr, Ga}$ ) series. These anomalies, reflected in the abnormal anisotropic increase of the thermal expansion coefficients with (several) maxima at the specific temperatures, are caused by thermally driven transitions from a low-spin (LS) to the excited spin states (IS or HS) of  $\text{Co}^{3+}$  ions and the coupled magnetic and metal-insulator transitions occurred in the systems. Clear signs of magnetoelastic coupling were discovered in  $\text{SmFeO}_3$  and some mixed RE ferrite perovskites, in which subtle deviations of the thermal expansion were observed at the magnetic ordering temperature  $T_N$ .

Several kinds of concentration and temperature-induced structural phase transitions and diverse sorts of lattice expansion anomalies have been detected in the RE-(Ni,Pd)-Ga intermetallic systems. In particular, diverse sequences of structural phase transitions were found in the  $\text{La}(\text{Ce})\text{Ni}_{13-x}\text{Ga}_x$  solid solution series. In  $\text{YbNiGa}$  and  $\text{YbPdGa}$  compounds, pronounced abnormal lattice expansion and negative thermal expansion phenomena were discovered in a broad temperature range of 8 K–1173 K.

**Acknowledgment.** The studies were supported in parts by the ICDD Grant-in-Aid Program and the research fellowship program of the Max-Planck Society (Germany).

- [1] L. Vasylechko, A. Senyshyn, U. Bismayer. Perovskites-Types Aluminates and Gallates; K.A. Gschneidner, Jr., J.C.G. Bünzli, V.K. Pecharsky, Eds.; Handbook on the Physics and Chemistry of Rare Earths. Elsevier, B.V.: Amsterdam, The Netherlands, 2009; Volume 39, pp. 113–295.



## Topological Transition in Quasi 2D-crystals

**B. Lukiyaneets\*, D. Matulka**

*Lviv Polytechnic National University, 12 Bandery St., 79013, Lviv, Ukraine*

*\*e-mail: [bohdan.a.lukiyaneets@lpnu.ua](mailto:bohdan.a.lukiyaneets@lpnu.ua)*

Recently, a number of works have appeared devoted to the study of quasi 2D-crystals, and in particular of layered crystals. Interest in them has been sharply revived after the discovery of graphene in 2004. Graphene is a monolayer of graphite. As an example of quasi 2D-crystals, layered crystals - graphite, dichalcogenides of transition metals)  $MX_2$ , semiconductors  $A_3B_6$  - are a set of monoatomic planes or packets of atoms connected by a covalent or ionic-covalent bonds, while the connection between the packets is carried out by a much weaker, namely van der Waals bond. Such dissimilar bonds are the reason for pronounced anisotropy in the physical characteristics of the quasi 2D-crystals, which can be widely modified by intercalation, hydrostatic compression, etc.

The dispersion law of a single-zone model of a quasi 2D-crystal, taking into account different types of chemical bonds in them, can be presented in the following form:

$$E(\vec{k}) = \frac{\hbar^2 k_{||}^2}{2m^* a_{||}^2} + 2\beta \sin^2\left(\frac{k_z a_z}{2}\right). \quad (1)$$

Here, the first term is the dispersion law of electron in the approximation of the effective mass in the plane of the layers, and the second one is the dispersion law along  $k_z$  in the strong bond approximation taking into account the electronic overlap between adjacent layers  $\beta_{vv+1} = \beta$  ( $v$  is the layer number,  $\vec{k}_{||}(k_x, k_y)$  is the 2D quasi-momentum,  $a_x, a_y, a_z$  are the lattice parameters. The width of the allowed zone along OZ,  $2\beta$ , is much smaller than the width of the allowed zone in the plane of the layers, XOY. It is this fact that can cause a topological transition (or Lifshitz transition) in quasi 2D-crystals.

The Lifshitz transition is a transition from a closed isoenergetic surface to an open one, when the Fermi level crosses the width of the allowed zone  $2\beta$ . A change in the position of the Fermi level, as shown in a number of works, can be implemented in various ways - by a strong magnetic field, by ultrashort laser pulses, due to electrons strongly interacting with photons, etc.

In the proposed work, the implementation of the topological transition is proposed using resonant irradiation in the frequency  $\Omega$ , which is determined by the condition  $0 < \hbar\Omega - E_g \ll E_g$  ( $E_g$  is the energy gap).

For this, a model quasi 2D-semiconductor with a valence band and a conduction band with dispersion laws of type (1) was considered. In the electromagnetic field, such zones are renormalized with the formation of quasiparticles electron-hole. Irradiation of such a semiconductor with an electromagnetic wave  $\Omega$  leads to a countershift of the renormalized zones, proportional to  $\Omega$ . Therefore, at a certain value  $\Omega$ , the Fermi level will be able to reach the topological transition point first of the first zone, and then the second one, or vice versa, depending on the relationship between the parameters  $\beta_c, \beta_v, m_c, m_v$ . As a result, the formation of a gap in the spectrum along  $k_z$ , which was possible before the topological transition, disappears.



# Supersymmetry and Entangled States in Quantum Optics

H. Laba<sup>1</sup>, V. Tkachuk<sup>2\*</sup>

<sup>1</sup>*Department of Applied Physics and Nanomaterials Science, Lviv Polytechnic National University*

<sup>2</sup>*Department for Theoretical Physics, Ivan Franko National University of Lviv,*

*\*e-mail: [voltkachuk@gmail.com](mailto:voltkachuk@gmail.com)*

Entanglement is an important resource in quantum information and quantum computing. On the other hand, supersymmetry is a powerful tool in quantum mechanics. Supersymmetry (SUSY) and entanglement in the Jaynes-Cummings model, which describes two levels of atoms interacting with one electromagnetic mode, have been examined in resonance cases when the transition energy between two levels is equal to the photon's energy. The total Hamiltonian of the Jaynes-Cummings model can be presented as a linear combination of supercharge and squared supercharge. The supercharge corresponds to the interaction between the atom and the photon. When interaction is absent, Hamiltonians possess SUSY, and nonzero energy levels degenerate twofold. Note that considering interaction in Hamiltonian leads to splitting of energy levels. In this case, the eigenstates of the Jaynes-Cummings model correspond to eigenstates of supercharge, and the entanglement of atom state with photon is maximal. The presentation is based on the publication [H. P. Laba, V. M. Tkachuk, Entangled states in supersymmetric quantum mechanics, Mod. Phys. Lett. A 35, No. 34, 2050282 (2020)].



# Control of Second-Harmonic Generation via Phase-Matched induced by Magnetization in Iron Garnet Epitaxial Thin Films

I. Syvorotka<sup>1</sup>, D. Guichaoua<sup>2\*</sup>, N. Syvorotka<sup>1</sup>, R. Wielgosz<sup>3</sup>, A. Andrushchak<sup>4</sup>, S. Taboukhat<sup>2</sup>, B. Sahraoui<sup>2</sup>

<sup>1</sup>Scientific Research Company "Electron-Carat", Lviv, Ukraine

<sup>2</sup>LPhIA Laboratory, University of Angers, Angers, France

<sup>3</sup>ENERGIA OZE Sp. z o.o Konopiska, Poland

<sup>4</sup>Lviv Polytechnic National University, Lviv, Ukraine

\*Tel: (+33) 241 735 219, e-mail: [d.guichaoua@univ-angers.fr](mailto:d.guichaoua@univ-angers.fr)

Bismuth-free yttrium iron garnet (YIG) magnetic films and bismuth-doped iron garnet (Bi:YIG) magnetic films were grown via the liquid phase epitaxy (LPE) method on single crystal substrates of gadolinium gallium garnet (GGG). The films grown demonstrated excellent crystalline and optical quality with a preferred (111) orientation. Both doped and undoped samples of bismuth exhibited lattice-mismatch strain, originating from anisotropic growth and differences in lattice parameters between the substrate and the film. This strain disrupted the inversion symmetry of the crystal and produced strain-induced SHG [1]. Magnetization properties were analysed at room temperature using a vibrating sample magnetometer (VSM). Hysteresis loops were measured both in-plane and perpendicular to the film plane to characterize the magnetic properties of the films. This was done by analysing lattice-mismatch strain, Faraday rotation, and the orientation of the spontaneous magnetization vector. Results showed that the Faraday rotation in bismuth-doped samples increased significantly compared to bismuth-free samples due to two to four diamagnetic transitions [2]. We examined SHG using the Maker fringes method. Although bismuth-free and bismuth-doped films did not exhibit SHG signal in transmission, only bismuth-doped films exhibited SHG [3,4]. The intensity of second harmonic generation was found to exhibit a correlation with the orientation of the spontaneous magnetization vector, with the maximum peak occurring at around 45°. We investigated the effects of an external magnetic field on second harmonic generation (SHG). The findings demonstrated a direct correlation between the intensity of the second harmonic and the magnitude of the external magnetic field, revealing the potential for modulation by external magnetic fields.

**Acknowledgment:** The presented results are part of IMAGE project that has received funding from the EU Horizon 2020 research and innovation program under the Marie Skłodowska-Curie grant agreement No 778156.

- [1] P. Kumar, A. Maydykovskiy, L. Miguel et al, *Opt. Express* 18, 1076-1084 (2010)
- [2] A. K. Zvezdin and V. A. Kotov, IOP, London, U.K., 1997
- [3] K. Iliopoulou, D. Kaspruwicz, A. Majchrowski et al., *Applied Physics Letters* 103 (23) 2013
- [4] S. Abed, H. Bougharraf, K. Bouchouit et al., *Superlattices and Microstructures* 85, 370-378 (2015)



## Generation of Acoustic Vortices and Acousto-Optic Interactions with Acoustic Vortex Beams

I. Martynyuk-Lototska, M. Kostyrko, D. Adamenko, I. Skab and R. Vlokh\*

*Vlokh Institute of Physical Optics, Dragomanov Str.,23, 79005 Lviv, Ukraine*

\*Tel: (032) 2611489, Fax: (032) 2611483, e-mail: [r\\_vlokh@ukr.net](mailto:r_vlokh@ukr.net)

In the present work, we have shown that the acoustic vortex beams can be generated with the aid of the acoustic spiral phase plate and the acoustic grating having the fork-like bifurcation of its slits [1]. The generation of the acoustic vortex beams has been revealed experimentally. Moreover, the effect has been proved by the influence of these beams on the particles floating on the water surface: the acoustic vortex beam leads to the rotation of these particles. We have found clear evidence that the intensity of the acoustic vortex beam increases from zero in its center to a certain maximal value near the edge of the vortex beam. Then the phase is changed by the angle  $2\pi$  rad whenever the azimuthal angle is changed by the same value.

We have studied the acousto-optic diffraction of the optical beam by the acoustic beam bearing the acoustic vortex. In the intermediate Bragg–Raman–Nath regime, each of the nonzero diffraction maximums is split into two maximums which correspond to diffraction by the elementary acoustic rays close to the edges of the acoustic vortex beam. At the same time, the dark region appearing in between these maximums is caused by destructive interference of the elementary optical rays produced due to diffraction by the opposite sides of the acoustic vortex beam, which are phase-shifted by  $\pi$  rad. Unfortunately, we have been not able to detect a transfer of the orbital angular momentum from the acoustic beam to the diffracted optical beam in the course of the acousto-optic diffraction.

[1] I.Martynyuk-Lototska et al. (2023) *Appl. Opt.* 62, 3643-3648.



# The Experimental Definition of Electro-optical Parameters in the LiTaO<sub>3</sub> Crystals. Analytical Representation of Spatial Anisotropy

B. Olkhovyk<sup>1</sup>, Y. Lozynskiy<sup>1</sup>, Z. Kohut<sup>1,2\*</sup>

<sup>1</sup>Lviv Polytechnic National University, 5 Ustyianovych str., 79005 Lviv Ukraine

<sup>2</sup>Czestochowa University of Technology, ul. Dąbrowskiego 69, 42-201 Częstochowa, Poland

\*e-mail: [zinoviy.o.kohut@lpnu.ua](mailto:zinoviy.o.kohut@lpnu.ua)

The interferometric method for investigating the electro-optic effect in LiTaO<sub>3</sub> crystals was applied using a Michelson interferometer setup. Additionally, two semi-transparent thin mirrors were used on each of the paths of the two reference beams. This prevented the separation and unwanted reflection of the reference beams, resulting in a higher intensity of the beam passing through the studied crystal. The overall interferometric pattern became clearer and more stable. This led to an increased accuracy in determining the electro-optic coefficients.

The electrically induced change  $\delta_{ikl}$  of the optical path of the light beam passing through the investigated sample, in the case of a two-pass interferometer, is caused by a change in the refractive index of this crystal (electro-optical effect) in the direction of light propagation under the applied electric field and it is determined by the dependence:

$$\delta(\Delta_{ikl}) = \frac{-r_{il}n_i^3}{2} E_l t_k + (n_i - 1) d_{lk} E_l t_k \quad (1)$$

It is possible to define the coefficients for the calculation of all effective EOCs for two cases of interferometric measurements. The EOE coefficients were calculated according to the general formula:

$$r_{ij} = -n_i^3 \frac{2\Delta}{E_l t_k} + 2n^3 (n_i - 1) d_{ik} \quad (2)$$

In the current study, we enhanced the previously suggested method by implementing the most accurate technique for tool adjustment. The proposed method in the experimental setup and mathematical dependencies makes it possible to determine all electro-optical coefficients in LiTaO<sub>3</sub> crystals based on the changes in the optical path measured with the help of electric field-induced stresses. The measurement results are given in the Table 1.

Indicative surfaces for the studied crystal (indicative surfaces in LiTaO<sub>3</sub> crystals) were constructed [2] using the provided dependencies:

| k | i | l  | r <sub>il</sub> | r, 10 <sup>-12</sup> m/B |
|---|---|----|-----------------|--------------------------|
| 1 | 3 | 3  | r <sub>33</sub> | 28,0 ± 2.0               |
| 1 | 3 | 3' | r <sub>33</sub> | 31.8 ± 2.0               |
| 1 | 2 | 3' | r <sub>13</sub> | 10.3 ± 0.5               |
| 1 | 2 | 3  | r <sub>13</sub> | 9.1 ± 0.5                |
| 2 | 1 | 3  | r <sub>13</sub> | 8.0 ± 0.5                |
| 2 | 1 | 3' | r <sub>13</sub> | 9.9 ± 0.5                |
| 2 | 3 | 3' | r <sub>33</sub> | 31.9 ± 0.5               |
| 2 | 3 | 3  | r <sub>33</sub> | 30.2 ± 0.5               |

Table 1. Table of measurements and calculations for a direct cut of LiTaO<sub>3</sub> crystals

$$r'_{il}(\theta, \varphi) = -r_{22} \sin^3 \theta \sin 3\varphi + (r_{13} + r_{51}) \sin^2 \theta \cos \theta + r_{33} \cos^3 \theta,$$

$$r'^{(i)}_{il}(\theta, \varphi) = -r_{22} \sin^2 \theta \cos 3\varphi,$$

$$r'^{(l)}_{il}(\theta, \varphi) = r_{22} \sin \theta \sin 3\varphi + r_{13} \cos \theta,$$

$$r'^{(k)}_{il}(\theta, \varphi) = -r_{22} \sin \theta \cos^2 \theta \sin 3\varphi + r_{13} \cos^3 \theta + (r_{33} - 2r_{51}) \sin^2 \theta \cos \theta$$

It made it possible to analyze the spatial anisotropy of the electro-optical effect in LiTaO<sub>3</sub> crystals and choose the most effective geometry use of these crystals.

[1] A.S. Andrushchak et al. (2009) *Opt.Lasers.End.* 47, 31-38.

[2] A.S. Andrushchak et al. Spatial anisotropy of induced optic effects in crystal materials. Lviv:Prostir-M, 2019. 200 P.



# Comparative Investigation of Nonlinear Optical Responses in Various Lanthanide Coordination Compounds

H. El Karout<sup>1,2\*</sup>, A.V. Kityk<sup>3</sup>, R. Wielgosz<sup>4</sup>, S. Taboukhat<sup>1</sup>, D. Guichaoua<sup>1</sup>,  
A. Andrushchak<sup>5</sup>, O. Krupka<sup>1</sup>, B. Sahraoui<sup>1</sup>

<sup>1</sup> University of Angers, LPHIA, SFR MATRIX, 2 Bd. Lavoisier, 49045 Angers Cedex 01, France

<sup>2</sup> University of Angers, MOLTECH Anjou - UMR CNRS 6200, Angers, France

<sup>3</sup> Czestochowa University of Technology, Al. Armii Krajowej 17, 42-200 Czestochowa, Poland

<sup>4</sup> Energia Oze Sp. z o.o., ul. Czestochowska 7, 42-274 Konopiska, Poland

<sup>5</sup> Lviv National Polytechnic University, 12 S. Bandery str., 79013 Lviv, Ukraine

<sup>6</sup> University of Angers, Laboratoire MINT, UMR INSERM U1066 // UMR CNRS 6021, France

\* e-mail: [houda.elkarout@univ-angers.fr](mailto:houda.elkarout@univ-angers.fr)

Recent advancements in the study of lanthanide coordination compounds have opened new avenues of exploration. These compounds, known for their distinctive optical, magnetic, and catalytic properties, have captured the interest of researchers across various fields, including materials science and biology [1-2]. Surprisingly, their potential in the realm of nonlinear optics (NLO) has been largely overlooked. This study focuses on investigating the NLO characteristics of lanthanide coordination compounds, particularly Europium (Eu) and Gadolinium (Gd) complexes, embedded in poly(methyl methacrylate) (PMMA) matrix. The research aims to explore both the linear and nonlinear optical properties of thin films composed of these composite materials. By conducting second- and third-order nonlinear optical response measurements, specifically second and third harmonic generations (SHG and THG), this study seeks to contribute valuable insights into the NLO potential of these compounds. Understanding their behavior in nonlinear optics could pave the way for the development of innovative materials for applications in optical devices and communication technologies.

**Acknowledgment:** The presented results are part of IMAGE project that has received funding from the EU Horizon 2020 research and innovation program under the Marie Skłodowska-Curie grant agreement No 778156.

- [1] C. Andraud, O. Maury. *European Journal of Inorganic Chemistry*. 2009. (29-30), 4357-4371.
- [2] Y. Hasegawa, Y. Wada, S. Yanagida. 2004, *Journal of Photochemistry and Photobiology C: Photochemistry Reviews*, 5 (3), 183-202.



# Computer Simulation Studies of Collective Dynamics in Complex Metallic Glasses and Ionic Melts

T. Bryk<sup>1,2\*</sup>

<sup>1</sup>*Institute for Condensed Matter Physics of NASU, 79011 Lviv, Ukraine*

<sup>2</sup>*Lviv Polytechnic National University, 79013 Lviv, Ukraine*

\*Tel: +380(322) 276 1978, e-mail: [bryk@icmp.lviv.ua](mailto:bryk@icmp.lviv.ua)

Vibrational dynamics in disordered systems such as glasses and liquids is one of the most fascinating problems of modern condensed matter physics. Collective excitations in liquids and glasses have many specific features not observed in crystalline solids [1,2,3]. For the case of liquids, the long-wavelength acoustic modes are governed by macroscopic conservation laws, resulting in hydrodynamic propagation of longitudinal sound and the absence of transverse sound excitations in the long-wavelength region of the spectrum [4]. For glasses, the particular features of collective dynamics are the emergence of nonergodicity upon glass transition and the Boson peak feature in the vibrational density of states [2]. Estimating dispersion laws of acoustic and high-frequency excitations in liquids and glasses from computer simulations allows us to rationalize the dynamic structure of disordered systems observed in Inelastic X-ray scattering (IXS) experiments.

I will talk about recent simulation results for collective dynamics in a three-component metallic glass ZrCuAl [1] and in ionic oxide melt Al<sub>2</sub>O<sub>3</sub>. I will show how analyzing time-dependent correlations observed in computer simulations allows us to discriminate between contributions from acoustic and optic-like excitations. This allows direct estimation of the dispersion of longitudinal and transverse collective excitations and comparison of their manifestation in the shape of dynamic structure factors measured in IXS experiments. In contrast to crystals, the optic modes in many-component liquids and glasses are overdamped. I will discuss the mechanism of damping for optic-like modes in liquids.

[1] T. Bryk, N. Jakse, G. Ruocco, J.-F. Wax (2022) *Phys. Rev. B.* 106, 174203.

[2] T. Bryk, I. Mryglod (2010) *Phys. Rev. B.* 82, 174205.

[3] T. Bryk, M. Kopcha, G. Ruocco (2023) *J. Molec. Liq.* 387, 122622.

[4] T. Bryk, G. Ruocco, A.P.Seitsonen (2023) *Sci. Rep.* 13, 18042.



# Vector Phase Matching in Orthorhombic Biaxial Crystals by Extreme Surface Method

D. Shulha, O. Buryy, A. Andrushchak

Lviv Polytechnic National University, 12 Stepana Bandery Str., 79013 Lviv, Ukraine

Tel: (0322) 258 2696, e-mail: [oleh.a.buryi@lpnu.ua](mailto:oleh.a.buryi@lpnu.ua)

Non-linear optical effects depend on the directions of input and output beams relative to the structure of a crystalline material. This means some angle combinations significantly increase frequency-mixing processes compared to others. Second Harmonic Generation (SHG), Sum Frequency Generation (SFG), and Difference Frequency Generation (DFG) are particular processes that are being explored. The scope of this paper was limited to crystals of orthorhombic syngony.

The most common and relatively simple way to ensure optimal orientations is by performing scalar phase matching (SPM) by making the input and output beam's angular frequency  $\omega$  meet the matching condition  $\omega_1 + \omega_2 = \omega_3$ . The directions of beams in SPM coincide for the case of uniaxial crystals, and for biaxial crystals usually consider the case of light propagating only in the principal planes, for a reason of simplification.

However, a more sophisticated and complicated way to ensure optimal directions is by performing a vector phase matching (VPM) by making the input and output beam's corresponding wave vectors  $\vec{k}$  meet the matching condition  $\vec{k}_1 + \vec{k}_2 = \vec{k}_3$ . Our approach for solving this problem is based on the construction and analysis of the extreme surface (see [1,2] for details) to represent the spatial anisotropy of non-linear optical effects. The thing is, for each given direction of an output beam's wave vector, plenty of input wave vectors satisfy matching conditions. For each pair of input wave vectors, generation efficiency will be different. Therefore, for each output beam direction, the maximal efficiency should be determined by the optimization procedure. The surface constructed when the direction of  $\vec{k}_3$  is changed within the full spherical angle reflects all possible maxima of the effect; the highest among them (the global one) takes place for wave vector directions optimal for the considered effect in a given crystalline material.

The determination of such optimal directions and the corresponding global maxima of SHG, SFG and DFG efficiencies was carried out for a number of uniaxial and biaxial optical crystals: KTP, KTA, KB5, KNbO<sub>3</sub>, LBO, CBO, LRB4. As it is shown, in a significant number of cases, the vector phase matching ensures significantly higher efficiencies than the scalar one.

**Acknowledgment:** These results are part of a project that has received funding from the EU Horizon 2020 research and innovation programme under the Marie Skłodowska-Curie grant agreement No 778156. This work was also supported by the Ministry of Education and Science of Ukraine in the frame of the project 'Nanoelectronics' (0123U101695).

[1] A. Andrushchak et al. (2017) Appl. Opt. 56, 6255-6262.

[2] O. Buryy et al. (2018) JOSA B. 36, 1839-1845.



**Section 3**

**NANOENGINEERING TECHNOLOGIES AND  
PROCESSES**





## Preparation of $\text{Bi}_{12}\text{GeO}_{20}$ Nanocrystalline Structures

Ya. Shchur<sup>1,2\*</sup>, V. Adamiv<sup>3</sup>, I. Teslyuk<sup>3</sup>, A. Andrushchak<sup>1</sup>

<sup>1</sup>Lviv Polytechnic National University, Lviv, 12 Stepan Bandera str., Lviv 79013, Ukraine

<sup>2</sup>Institute for Condensed Matter Physics, 1 Svientsitskii str., Lviv 79011, Ukraine

<sup>3</sup>O.G. Vlokh Institute of Physical Optics, 23 Dragomanov str., Lviv 79005, Ukraine

\*e-mail: [ya.shchur@gmail.com](mailto:ya.shchur@gmail.com)

The problem of creating new functional materials with adjustable optical properties used in membrane technologies, optics, quantum electronics, analytical instrumentation, and photonics is of great importance. The so-called porous glasses are promising matrices for such materials due to their unique set of adsorption, diffusion, optical, and other characteristics combined with adjustable structural parameters of the nanoscale range [1,2]. When substances with active physical properties are introduced into porous matrices, the functional capabilities of the introduced components are significantly expanded and the practical significance of such structures increases significantly [3,4].

In our studies, we use nanoporous  $\text{Al}_2\text{O}_3$  and Si membranes, both purchased from SmartMembranes (Germany) and membranes manufactured by ourselves at the same company.

The polycrystalline fine powder  $\text{Bi}_{12}\text{GeO}_{20}$  (BGO) was applied to the surface of the Si and  $\text{Al}_2\text{O}_3$  samples and evenly distributed on its surface. Pieces of the single-crystal BGO sample were preliminarily crushed mechanically and carefully ground in an agate mortar for several hours to a fine powder. The nanocrystalline matrices were pre-annealed at a temperature of  $\sim 200^\circ\text{C}$  to purify them from foreign organic compounds.

The melting of BGO powder on the surface of Si and  $\text{Al}_2\text{O}_3$  matrices was carried out in a muffle resistive furnace at a temperature of  $950^\circ\text{C}$ . The matrices were kept at this temperature for 30 min to saturate the pores with BGO melt. Further crystallization took place during spontaneous cooling in a switched-off furnace. It is important to choose a substrate for nanoporous matrices, which, in the case of melt "leakage," will allow separation of the nanocrystalline structure from the substrate. We used mica plates.

As a result of the synthesis of BGO in the pores of Si and  $\text{Al}_2\text{O}_3$  matrices, it was found that the  $\text{Al}_2\text{O}_3$  matrix practically crumbled. X-ray diffraction analysis showed that  $\text{Al}_2\text{O}_3$  crystallized and cracked. While in the pores of the Si matrix, the formation of the BGO crystal structure was confirmed.

**Acknowledgment:** This work has received funding from the National Research Foundation of Ukraine (Project 2021.01/0410) and from the European Union's Horizon 2020 research and innovation programme under the Marie Skłodowska-Curie grant agreement No.778156.

- [1] A. Huczko (2000) *Applied Physics A* 70, 365-376.
- [2] P. Göring and M. Lelonek (2018) Highly ordered porous materials in *Nanoscience and Nanotechnology*, Marcel Van de Voorde, Ed., De Gruyter, Berlin.
- [3] O. Yaremko et al. (2019) AICT-2019: proceedings of the 3rd International conference, Lviv, Ukraine, 96–100.
- [4] O. Yaremko, et al. (2022) Proceedings of the 16th IEEE TCSET Lviv-Slavske, Ukraine, 689-693.



## Structures of InSb for Infrared Photodiodes Obtained by the Method of Pulsed Cooling of a Saturated Solution-Melt

M. Vakiv<sup>1</sup>, S. Krukovskiy<sup>1\*</sup>, I. Iznin<sup>1</sup>, J. Kost<sup>2</sup>, V. Arikov<sup>2</sup>, O. Kulbachynskiy<sup>3</sup>,  
O. Gudymienko<sup>3</sup>, O. Dubikovskiy<sup>3</sup>

<sup>1</sup>Scientific research company "ELECTRON-CARAT", 202 Stryyska Str, Ukraine

<sup>2</sup>Lviv Polytechnic National University, 12 Stepan Bandera Str, Ukraine

<sup>3</sup>V.E. Lashkaryov Institute of Semiconductor Physics NAS of Ukraine, 41 Nauki Ave

\*Tel: (+38) 096 839 8370, e-mail: [goro0609@gmail.com](mailto:goro0609@gmail.com)

Indium antimonide, together with a solid solution of  $\text{Cd}_x\text{Hg}_{1-x}\text{Te}$ , is the main material for the manufacture of photodiodes in the range of 3–5.5  $\mu\text{m}$ . With practically the same basic parameters of photodiodes (sensitivity, specific detection ability), the advantages of InSb are primarily related to the greater thermal stability of the material and uniformity and lower cost. This stimulates research on improving the technology of instrument structures based on InSb. LPE provides the most balanced conditions for obtaining epitaxial structures based on InSb. However, the high solubility of Sb at low temperatures significantly complicates the technology of forming thin InSb epitaxial layers with a thickness of 1-3  $\mu\text{m}$ , which are optimal for achieving high sensitivity of photodetectors. The purpose of this work was to conduct research on obtaining device structures based on InSb using the method of pulsed cooling of a saturated solution-melt, which ensures the formation of layers of submicron and nanoscale thicknesses.

The change in the amount of supercooling at the crystallization front of the indium solution-melt-indium antimonide substrate was calculated depending on the epitaxy notch temperatures and the temperature of the cold body. Based on this, it was experimentally established that layers of indium antimonide with a thickness of 1-3 microns can be crystallized at temperatures in the range (405-420) °C.

To reduce the level of background impurities in the InSb layers, the method of complex alloying with microconcentrations of the rare earth element gadolinium and isovalent gallium developed in [1] was used. It was established that at concentrations of cadmium in the indium melt solution (0.0001-0.002) at% and dysprosium at 0.1 at%, p-type indium antimonide epitaxial layers with a hole concentration from  $8 \cdot 10^{14} \text{ cm}^{-3}$  to  $5 \cdot 10^{17} \text{ cm}^{-3}$  are crystallized.

X-ray structural measurements were carried out on a PANalytical X'Pert PRO - MRD diffractometer. Cu K $\alpha$  radiation (wavelength  $\lambda = 0.15406 \text{ nm}$ ) was used. It was determined that the lattice parameter of the epitaxial layer is equal to the lattice parameter of the substrate. Based on the analysis of 2 theta-omega scans of reflexes (111) and (333), no diffuse scattering asymmetry was detected. This shows that there are no residual deformations (either stretching or compression) in the film.

The study of volt-ampere characteristics, mesa-structures of test samples of photodiodes made on the basis of the p-InSb/n-InSb epitaxial structure proved that the reverse current at a temperature of (80 $\pm$ 2) K does not exceed the value of  $1 \cdot 10^{-7} \text{ A}$ .

The promising application of the method of pulsed cooling of a saturated solution-melt for obtaining InSb structures with layers of micron and submicron thicknesses has been demonstrated.

- [1] S. I. Krukovskiy, V. Popov, R. Savkina, A. Smirnov (2004) *The European Physical Journal Applied Physics*. 27, 177–179.



# Study of Coloumb Correlation Influence on SPPs Frequency Spectrum in Dielectric/Metal/Dielectric Structures

P.P. Kostrobii<sup>1</sup>, V.Ye. Polovyi<sup>1\*</sup>, O.Y. Pits<sup>1</sup>

<sup>1</sup>Lviv Polytechnic National University, 12 Stepana Bandery str, Lviv, Ukraine

\*e-mail: [vitalii.y.polovyi@lpnu.ua](mailto:vitalii.y.polovyi@lpnu.ua)

This paper delves into the study of dielectric/metal/dielectric structures, particularly when the metal is an atomically thin film (further referred to as ATMF) with a thickness of up to 100nm. We conducted simulations focusing on the propagation of surface plasmon polariton (SPP) waves within these structures. The structural setup comprises two dielectric layers with an ATMF sandwiched between them. The chosen coordinate system positions the XOY plane to divide the ATMF into two equal parts. The SPP wave is assumed to propagate along the X-axis. For the dielectric materials, we consider high-frequency approximations, making their permittivity functions of time or frequency. However, the dielectric permittivity of the metal varies with both time and spatial coordinates, allowing us to account for spatial dispersion in the ATMF region. In this scenario, the interconnection between electric field vectors denoted as  $\epsilon_1(\omega)$  and  $\epsilon_3(\omega)$ , exhibits non-local behavior due to the non-stationary nature of the process under investigation. Furthermore, we specifically examine the case of transverse magnetic (TM) polarization of the field strength vectors  $\epsilon_1(\omega)$  and  $\epsilon_3(\omega)$ , as it is established that surface plasmon polaritons (SPPs) are present under this polarization configuration [1].

We conducted a study on the model for the following structures: "SiO<sub>2</sub>/Ag/Si," "Vacuum/Ag/Si," and "Vacuum/Ag/Al<sub>2</sub>O<sub>3</sub>" [1, 3]. The findings revealed that even a somewhat rudimentary consideration of Coulomb correlations, specifically their impact on the chemical potential, results in noteworthy alterations to the frequency spectrum of Surface Plasmon Polaritons (SPPs) when compared to the conventional approach that correctly addresses the condition of electroneutrality for a non-interacting electron system. This can be attributed to the fact that in the context of an interacting system, the influence of quantum size effects becomes significantly more pronounced. The characteristic oscillation pattern of the spectrum, stemming from the discrete energy levels, gradually diminishes as the film thickness increases. This phenomenon aligns with the known behavior of the chemical potential [3]. Furthermore, the rate at which the oscillation peaks decay is largely contingent on the Wigner-Seitz radius [4]. It's important to highlight that the spectrum's dependence on the dielectric environment surrounding the atomically thin metal film (ATMF) should not be overlooked. Crucially, the incorporation of Coulomb correlations also results in a marked improvement in the agreement with experimental data, underscoring the importance of considering these correlations when modeling the propagation of SPP waves in ATMF.

- [1] S. Ali Hassani Gangaraj and F. Monticone (2019) *Optica*. 6, 1158-1165.
- [2] P. Kostrobij, B. Markovych (2018) *Philosophical Magazine Letters*, 98, 21, 1991-2002.
- [3] V. Pogosov, A. Babich, and P. Vakula, *Phys. Solid State* 55, 2120.
- [4] N. Ashcroft, N. Mermin (1976) *Cornell University, Harcourt*, Solid State Physics



# Multi-qubit Quantum Graph States and Studies of their Properties with Quantum Programming

**Kh. P. Gnatenko**

*Ivan Franko National University of Lviv, Professor Ivan Vakarchuk Department for Theoretical Physics, 12 Drahomanov St., Lviv, 79005, Ukraine*

*\*e-mail: [khrystyna.gnatenko@gmail.com](mailto:khrystyna.gnatenko@gmail.com)*

Quantum states that can be associated with graphs are known as quantum graph states. The states are entangled and have a clear structure with graph representation. Therefore, they play an important role in quantum information and quantum programming, for instance, in quantum error correction algorithms, quantum cryptography, and others.

We consider quantum graph states of spin systems with Ising interaction [1,2]. The states can be associated with graphs considering spins as vertices and interactions between them as edges. The geometric measure of entanglement of the states, as well as geometric properties, were studied. We obtained a relation for the geometric measure of entanglement of a spin with other spins in the states with the degree of vertex representing it in the graph. We also found the relation of the geometric characteristics, namely the velocity of quantum evolution, the curvature, and the torsion of the quantum graph states with graph properties. They are the total number of edges, triangles, and squares in the corresponding graphs.

Quantum protocols for the detection of the geometric measure of entanglement and geometric properties of the graph states were constructed. The protocol for studies of the geometric measure of entanglement is based on its relation with the mean spin obtained in the paper [3]. Detection of the geometric properties of the evolutionary quantum graph states with quantum programming is based on their relation with fluctuations of energy presented in [4]. Quantum protocols were performed on IBM's quantum devices. We calculated the geometric characteristics on quantum computer ibmq-atenth for particular cases of quantum graph states that correspond to a chain, a triangle, or a square. The results of quantum calculations are in agreement with theoretical ones. The proposed quantum algorithms open a possibility to achieve quantum supremacy with the development of multiqubit quantum devices.

We also consider quantum graph states generated by the action of controlled phase shift operators on a quantum state in which all the qubits are in arbitrary identical states. The geometric measure of entanglement of the states was calculated for arbitrary graph structure. We found the relation of the entanglement with parameters of the state and degree of the corresponding vertex [5].

The geometric measure of entanglement was calculated with quantum programming for states corresponding to different graph structures (complete graph, claw, chain, graph with structure of ibmq-valencia device). The results of quantum programming are in good agreement with analytical ones.

- [1] Kh. P. Gnatenko, V. M. Tkachuk (2021) *Phys. Lett. A* 396, 127248 [5 p.].
- [2] Kh. P. Gnatenko, H. P. Laba, V. M. Tkachuk (2022) *Phys. Lett. A* 452, 128434 [6 p.].
- [3] A. M. Frydryszak, M. I. Samar, V. M. Tkachuk (2017) *Eur. Phys. J. D* 71, 233 [8 p.].
- [4] H. P. Laba, V. M. Tkachuk (2017) *Condens. Matter Phys.* 20, 13003 [7 p.].
- [5] Kh. P. Gnatenko, N. A. Susulovska (2021) *EPL (Europhys. Lett.)* 136, 40003 [8 p.].



# Modeling the Separation Surface Influence on the Lattice Structure in Nanosystems

P. Kostrobij, I. Ryzha\*, M. Sheremeta

Lviv Polytechnic National University, St. Bandera str. 12, 79013 Lviv, Ukraine

\*Tel: 38 (032) 258 23 68, e-mail: [iryha.a.ryzha@lpnu.ua](mailto:iryha.a.ryzha@lpnu.ua)

Achievements in the development of nanotechnology led to a sharp increase in research aimed at building models that adequately describe numerous experimental studies of nanosystems [1]. Since modern, experimentally obtained nanosystems are characterized by dimensions of the order of 10 nm, their physical properties strongly depend on the dimensions (the so-called "quantum-size effect") [2]. One such characteristic is the density of the ionic subsystem, which can vary near the "metal–vacuum" separation surface. This change is caused by the presence near the separation surface (in the vacuum region) of a near-surface electronic layer [2], the thickness of which reaches the order of two lattice periods. This, in turn, leads to a change in the discrete lattice structure of the ionic subsystem. To describe such a change, we use the proposed quantum-statistical approach to modeling metallic systems with a "metal–vacuum" separation surface [2]. The use of this approach made it possible to obtain an effective Hamiltonian of the ionic subsystem in the approximation of pairwise interactions between ions:

$$H = H_0 + \sum_{n=1}^N \Phi_1(\vec{R}_n) + \sum_{n,n'=1}^N \Phi_2(\vec{R}_n, \vec{R}_{n'}), \quad (1)$$

where  $H_0 = \sum_{n=1}^N \frac{P_n^2}{2M}$  is the Hamiltonian of free ions with mass  $M$  and momentum  $\vec{P}_n$  ( $P_n \cdot d \ll 1$ ,  $d$  is the lattice period);  $N$  is the number of ions in the lattice structure;  $\Phi_1(\vec{R}_n)$  and  $\Phi_2(\vec{R}_n, \vec{R}_{n'})$  are, respectively, the single-particle potential (the appearance of which is caused by the electron–ion interaction) and the potential of the pairwise effective interaction between ions;  $\vec{R}_n$  is the radius vector describing the position of an ion in the lattice structure.

By substituting  $\vec{R}_n = \vec{R}_n^0 + \vec{\xi}_n$  into (1), where  $\vec{R}_n^0$  is the radius vector of an ion in the absence of a separation surface, we calculate the free energy  $F$  of model (1) in the quadratic approximation for  $|\vec{\xi}_n|$  and, from the condition

$$\vec{\nabla}_{\vec{\xi}} F = 0, \quad (2)$$

obtain and solve the equation for displacements  $\vec{\xi}_n$  that minimize the free energy  $F$ .

We obtain expressions for the diagonal component of the stress tensor  $\sigma_{ik}$ , taking into account the conditions of equilibrium on the surface. This allows us to calculate the change in the volume of the unit cell of the near-surface ionic layers, which in turn allows us to obtain a change in the density of ions in the near-surface region of the metal.

- [1] T. Nagirnyi, K. Tchervinka (2014) Basics of mechanics of local non-homogeneous elastic bodies. Bases of nanomechanics. II, Rastr-7, Lviv (in Ukrainian).
- [2] M. Vavrukh, P. Kostrobij, B. Markovych (2017) Basis approach in the theory of multi-electron systems, Rastr-7, Lviv (in Ukrainian).



## Functionalised Selected Conjugated Compounds for Nonlinear Optical Applications

B. Sahraoui<sup>1,\*</sup>, H. Karout<sup>2</sup>, A. A.V. Kityk<sup>3</sup>, Y. Shchur<sup>4</sup>, A. Andrushchak<sup>5</sup>,  
R. Wielgosz<sup>6</sup>, O. Kityk<sup>6</sup>, M. Lelonek<sup>7</sup>, P. Göring<sup>7</sup>, O. Krupka<sup>1</sup>

<sup>1,2</sup>University of Angers, LPHIA, SFR MATRIX, 2 Bd. Lavoisier, 49045 Angers, France

<sup>3</sup>Czestochowa University of Technology, Al. Armii Krajowej 17, 42-200 Częstochowa, Poland

<sup>4</sup>Institute for Condensed Matter Physics, 1 Svientsitskii str., 79011 Lviv, Ukraine

<sup>5</sup>Lviv National Polytechnic University, 12 S. Bandery str., 79013 Lviv, Ukraine

<sup>6</sup>Energia Oze Sp. z o.o., ul. Częstochowska 7, 42-274 Konopiska, Poland

<sup>6</sup>Ivan Franko National University of Lviv, 1 Universytetska St., Lviv, 79000, Ukraine

<sup>7</sup>SmartMembranes, Heinrich-Damerow-Str. 4, Halle (Saale) 06120, Germany

<sup>8</sup>University of Angers, Laboratoire MINT, UMR INSERM U1066 // UMR CNRS 6021, France

\*e-mail: [bouchta.sahraoui@univ-angers.fr](mailto:bouchta.sahraoui@univ-angers.fr)

Innovative optoelectronic devices for optical communications, optical switching, optical data information storage and optical limiting require an important development of materials based on molecular engineering of advanced molecular systems with exceptional nonlinear optical (NLO) responses<sup>[1]</sup>. There is great interest in developing such photonics systems, including self-assembled architectures for nonlinear optical applications and optoelectronics applications<sup>[2-5]</sup>. Molecular engineering is crucial for obtaining new photonics self-assembled architectures such as highly conjugated compounds based on supramolecular systems chemistry. In this talk, NLO properties of highly conjugated compounds based on supramolecular chemistry will be discussed in view of their optoelectronics applications<sup>[4]</sup> using powerful experimental techniques tools such as SHG, THG, and Z-Scan. Moreover, some interesting results on the anisotropic confinement of chromophores that induce second-order nonlinear optics in a nanoporous photonic metamaterial [5] will also be discussed. The obtained properties provide a unique assemblage for exploring interactions in newly designed smart membranes [5]. Moreover, a comparison between the obtained experimental NLO results and theoretical quantum chemical calculations will be discussed.

**Acknowledgments:** the presented results are part of IMAGE project that has received funding from the EU Horizon 2020 research and innovation program under the Marie Skłodowska-Curie grant agreement No 778156.

- [1] N. Paras Prasad, Book, *Nanophotonics*, ISBN-13: 978-0471649885 (2004).
- [2] A. Szukalski, P. Krawczyk, B. Sahraoui, F. Rosińska, and B. Jędrzejewska, *The Journal of Organic Chemistry*, 87, 7319–7332 (2022).
- [3] A. Szukalski, P. Krawczyk, B. Sahraoui, and B. Jędrzejewska. *The Journal of Physical Chemistry B*, 126, 1742–1757 (2022).
- [4] K. Waszkowska, Y. Cheret, A. Zawadzka, A. Korcala, A. El-Ghayoury, A. Migalska-Zalas, and B. Sahraoui, *Dyes And Pigments*, Vol. 186, N° 109036 (2021).
- [5] K. Waszkowska, P. Josse, C. Cabanetos, Ph. Blanchard, B. Sahraoui, D. Guichaoua, I. Syvorotka, O. Kityk, R. Wielgosz, P. Huber, A. Kityk, *Optics letters*, Vol. 46, Issue 4, pp. 845-848 (2021).



# Silica-Benzil and Alumina-Benzil Crystalline Nanocomposites: Textural Morphology and Nonlinear Optical Characterization

A.V. Kityk<sup>1\*</sup>, H. El Karout<sup>2</sup>, B. Sahraoui<sup>2</sup>, Y. Shchur<sup>3</sup>, A. Andrushchak<sup>4</sup>,  
R. Wielgosz<sup>5</sup>, O. Kityk<sup>5</sup>, J. Jędryka<sup>1</sup>, Y. Slyvka<sup>6</sup>, M. Lelonek<sup>7</sup>, P. Göring<sup>7</sup>,  
P. Huber<sup>8</sup>

<sup>1</sup>Czestochowa University of Technology, Al. Armii Krajowej 17, 42-200 Częstochowa, Poland

<sup>2</sup>University of Angers, LPHIA, SFR MATRIX, 2 Bd. Lavoisier, 49045 Angers Cedex 01, France

<sup>3</sup>Institute for Condensed Matter Physics, 1 Svientsitskii str., 79011 Lviv, Ukraine

<sup>4</sup>Lviv National Polytechnic University, 12 S. Bandery str., 79013 Lviv, Ukraine

<sup>5</sup>Energia Oze Sp. z o.o., ul. Częstochowska 7, 42-274 Konopiska, Poland

<sup>6</sup>Ivan Franko National University of Lviv, 1 Universytetska St., Lviv, 79000, Ukraine

<sup>7</sup>SmartMembranes, Heinrich-Damerow-Str. 4, Halle (Saale) 06120, Germany

<sup>8</sup>Hamburg University of Technology and Deutsches Elektronen-Synchrotron DESY,  
Notkestr. 85, 22607 Hamburg, Germany

\*Tel: (48 34) 325 0815, Fax: (48 34) 325 0823, e-mail: [andriy.kityk@pcz.pl](mailto:andriy.kityk@pcz.pl)

Nanocomposites provide entirely novel opportunities for optoelectronic and photonic applications. However, their synthesis often includes sophisticated top-down nanotechnologies to tailor textural morphology and, thus, the resulting nonlinear optical properties. We demonstrate a series of silica-benzil and alumina-benzil nanocomposites representing the mesoporous silica or alumina (anodic alumina oxide) templates and benzil nanocrystals embedded by capillary crystallization into their tubular nanochannels (6-300 nm). One aims to design novel, efficient nonlinear optical (NLO) composite materials in which the tubular scaffold structure of the host matrix provides mechanical robustness, whereas NLO functionality results from specific properties of the deposited guest nanocrystals.

In terms of symmetry, the benzil crystal is identical to crystal quartz; hence, it is characterized by piezoelectricity and specific parametrical and NLO properties. The high NLO efficiency of benzil crystals, in combination with high laser damage threshold, enhanced saturation absorption and negative nonlinear refractive index, make them favourable for laser frequency conversion applications such as second (SHG) and third (THG) harmonic generation. Benzyl has significant advantages over its inorganic counterpart, trigonal quartz. Due to its low melting point, benzyl nanocrystals can be easily melted and deposited in nanochannels. Its further solidification during cooling leads to the formation of a texture consisting of crystalline nanoclusters separated by voids. X-ray diffraction technique was used to characterize the texture morphology of silica- and alumina-benzil nanocomposites.

Spatial confinement significantly influences NLO features of both silica- and alumina-benzil nanocomposites being explored in SHG experiments. Multiply scattering and light depolarization on randomly distributed benzil nanoclusters considerably reduce the anisotropy of the SHG response. SHG response rises by more than three orders of magnitude as the channel diameter increases from 6.0 to 300 nm. It vanishes, on the other hand, when spatial cylindrical confinement approaches sizes of few molecular layers, suggesting thus that embedded benzil clusters indeed are not uniformly crystalline but are characterized by more complex morphology consisting of disordered SHG-inactive amorphous shell, covering the channel wall, and SHG-active crystalline core. Understanding and controlling the textural morphology in inorganic-organic nanocrystalline composites and its relationships with NLO properties can lead to the development of novel efficient NLO materials for light energy conversion with prospective optoelectronic and photonic applications.



## Effect of Photogeneration on Concentration of Excess Carriers in Si and Ge Crystals

A. Danylov<sup>1</sup>, B. Venhryn<sup>1\*</sup>, S. Luniov<sup>2</sup>, A. Korolyshyn<sup>3</sup>, I. Senko<sup>1</sup>,  
D. Afanassyev<sup>1</sup>, A. Ratych<sup>1</sup>, A. Andrushchak<sup>1</sup>

<sup>1</sup>Lviv Polytechnic National University, 12 Stepana Bandery str., 79013 Lviv, Ukraine

<sup>2</sup>Lutsk National Technical University, 75 Lvivska str., 43018 Lutsk, Ukraine

<sup>3</sup>Ivan Franko National University of Lviv, 8 Kyrylo and Mefodij str., 79005 Lviv, Ukraine

\*e-mail: [bohdan.y.venhryn@lpnu.ua](mailto:bohdan.y.venhryn@lpnu.ua)

Photogeneration of carriers in high resistivity Si and Ge is used to control the electromagnetic radiation in sub-THz and THz frequency ranges [1-3]. Change in carriers' concentration results in the formation of regions with either high absorption or high reflection of the abovementioned frequencies. Also, this effect is employed in developing high-speed switches based on coplanar waveguides [4]. Therefore, the studies on the effect of photogeneration on the concentration of excess carriers in Si and Ge are of particular importance. One should note that most theoretical calculations of this effect are currently available [3].

The present paper deals with the experimental determination of the effect of photogeneration on the concentration of the excess carriers in Si and Ge crystals. The authors use the approach to derive the concentration of photogenerated excess carriers from the photocurrent measurement at different light intensities, starting from zero (dark current), as explained in [5]. Here, one needs to know such quantities as equilibrium concentrations of electrons and holes, the ratio of their mobilities, and diffusion length for the samples under study. Resistivity and Hall effect measurements can determine these before the photoconductivity experiment. Particularly, equation (1) gives the concentration of photogenerated electrons (for an n-type semiconductor)  $\Delta N_e^I$  for a given light intensity  $i$  in the case of nonuniform light absorption ( $\alpha \cdot d \gg 1$ , a likely situation here):

$$\Delta N_e^I = \left( \frac{L}{d} \cdot \frac{I_i}{I_0} - 1 \right) \cdot (N_e \cdot b + N_p) / (1 + b) \quad (1)$$

where  $\alpha$  is the absorption factor,  $d$  is material thickness,  $L$  is the diffusion length,  $I_0$  is the dark photocurrent  $I_i$  is that at the light intensity  $i$ ,  $b = \mu_e / \mu_p$ ,  $\mu_e$  and  $\mu_p$  are respective mobilities of electrons and holes,  $N_e$  and  $N_p$  are their equilibrium concentrations.

The Si and Ge samples studies were the 0.5 mm thick square wafer pieces of  $p$ - and  $n$ -type 20x20 mm<sup>2</sup> in size. Their resistivity was in the range of 0.2 to 20 kOhm·cm. The preliminary characterization of these samples was carried out using the HMS-3000 Hall Measurement System, while the photocurrent measurements were performed in a 2-terminal configuration with a custom setup containing a high-power 565nm LED with controllable output as a light source.

**Acknowledgment.** This work was supported by the National Research Foundation of Ukraine (project #2021.01/0410).

- [1] H. Alius, G. Dodel (1991) *Infrared Phys.* 32, 1-11.
- [2] T. Vogel et al. (1992) *Appl. Opt.* 31, 329-337.
- [3] A. Kannegulla et al. (2015) *Opt. Express* 23, 32098-32112.
- [4] Y. Shi et al. (2021) *OSA Continuum* 4, 2642-2654.
- [5] R.A. Smith Semiconductors, 2<sup>nd</sup> edition, Cambridge Univ. press 1978, 523p.

## **Section 4**

# **APPLICATIONS OF INNOVATIVE MATERIALS**





## Development of sub-THz Modulators. Experience and Results

Y. Yashchyshyn<sup>1\*</sup>, V. Hajduchok<sup>2</sup>, S. Krukowski<sup>2</sup>,  
P. Bajurko<sup>1</sup>, J. Sobolewski<sup>1</sup>

<sup>1</sup>Warsaw University of Technology, Nowowiejska 15/19, 00-665 Warsaw, Poland

<sup>2</sup>Scientific Research Company CARAT - Branch Enterprise of PJSC Concern  
– ELECTRON (CARAT), Stryjska 202, 79031 Lviv, Ukraine

\*Tel: (4822) 234 77 27, e-mail: [yevhen.yashchyshyn@pw.edu.pl](mailto:yevhen.yashchyshyn@pw.edu.pl)

Devices based on photoconductive materials are promising solutions for future millimeter-wave electronic systems. So far, several examples of photoconductive microwave modulators/switches exist in the literature. However, their operating frequency and performance are low compared to other switching techniques [1]. In this paper, we propose photoconductive modulator/switch topologies based on the coplanar waveguide (CPW), which is more suitable for millimeter-wave applications than the published solutions, e.g. [2]. The utilization of low-temperature gallium arsenide (LT GaAs) as the photoconductive element is evaluated. Compared to epitaxial gallium arsenide (GaAs) grown at regular temperature, low-temperature epitaxial growth of LT GaAs results in a dramatically shorter carrier lifetime. This produces subpicosecond device responses and enables ultra-high-speed photodevices. LT GaAs is the most widely used material for fabricating photoconductive THz emitters or detectors. Its unique properties are good carrier mobility, high dark resistivity, and subpicosecond carrier lifetimes [3].

The device's construction consists of a grounded CPW line section on a two-layer substrate [4]. The top layer, directly under the signal and side conductors, is a 6  $\mu\text{m}$  thick layer of LT GaAs. The bottom layer is made of a 400  $\mu\text{m}$  thick Quartz dielectric. The purpose of the thick Quartz layer is to act as a mechanical support for the thin LT GaAs layer while providing the path for the beam of light activating the LT GaAs layer. To evaluate the influence of LT GaAs conductivity changes on the transmission of the mm-wave signal in the CPW, full-wave electromagnetic simulations utilizing the finite-difference time-domain (FDTD) method were carried out using CST Microwave Studio software. The length of a model is equal to 2.5 mm. All conductive elements are modeled as a 0.7  $\mu\text{m}$  thick copper layer. The transmission line section in the model was terminated with 50  $\Omega$  impedance excitation ports on both ends to calculate the full scattering matrix.

The influence of the photoconductive substrate conductivity changes on the transmission and reflection characteristics of the coplanar waveguide was investigated. Additionally, the feasibility of the utilization of thin-film photoconductive materials in the proposed switch was examined.

**Acknowledgment:** this work is part of a project IMAGE that has received funding from the European Union's Horizon2020 research and innovation programme under the Marie Skłodowska-Curie grant agreement No. 778156.

- [1] A. Fisher, Z. V. Missen, A. Semnani, D. Peroulis, arXiv:2012.07818v2, 20 Jul 2021.
- [2] J. Sobolewski, Y. Yashchyshyn, *IEEE ACCESS*, Vol. 10, 2022, pp. 12983-12999.
- [3] <https://www.powerwaywafer.com/lt-gaas.html>
- [4] J. Sobolewski, Y. Yashchyshyn, D. Vynnyk, V. Haiduchok, N. Andrushchak (2022), *ACTA PHYSICA POLONICA A* No. 4 Vol. 141.



## Polymer-Containing Composites for Li<sup>+</sup> Intercalation Current Generation

**O. Balaban\*, N. Mitina, A. Zaichenko, O. Izhyk**

*Lviv Polytechnic National University, 12 St. Bandery str., Lviv, 79013, Ukraine*

*\*Tel: (032) 258 2708, e-mail: [oksana.v.balaban@lpnu.ua](mailto:oksana.v.balaban@lpnu.ua)*

The issue of energy supply is currently of paramount importance not only in Ukraine but worldwide, alongside challenges in the field of micro and nanoelectronics materials and optics, which require immediate attention. The development of new nanocomposite materials, driven by increasing demands for high-performance energy storage, has become a vital focus of both fundamental and practical research. This relevance is evident in numerous endeavors aimed at achieving high charge capacity, low charge transfer resistance in electrode materials, rapid lithium ion diffusion within them, high cyclic capacity, and stability of lithium-based power sources.

On the other hand, the pressing concern today extends beyond enhancing the efficiency of these materials. There is also a need to reduce their cost and environmental impact. That is why functional materials of artificial origin, notably polymers, have emerged as highly versatile candidates for energy and electronic devices. As a result of persistent efforts, nanostructures have been synthesized, which consist of nanoparticles or nanofibers coated with an external inorganic or organic shell, or polymer composite films. These polymer shells or films serve various functions such as improving dispersion or interaction with the working environment, acting as a matrix for reinforcement, protecting against moisture or contaminants, and providing necessary electrical conductivity, energy storage, and more. Nevertheless, the reliable attachment of these shells to different surfaces while concurrently controlling their physicochemical properties presents a formidable challenge.

An exquisite blend of functionality and aesthetics can be achieved through the synthesis of polymeric organic-inorganic composites and coatings. The grafting of polymer brushes onto inorganic surfaces enables the formation of novel composite architectures, with the material's properties being heavily influenced by this process. Furthermore, polymers are easier to modify to obtain the desired properties, including the grafting of new polymer brushes on the surface or within the volume and incorporating various nanoparticles. Precise control over polymer coating thickness, composition, brush length, and density further enhance the ability to manipulate functional properties, paving the way for diverse practical applications.

Contemporary methods do not fully enable the production of polymer films with controlled height, porosity, or varying chemical composition. They require specific technological equipment and do not allow precise control over the process of obtaining polymer shells on the surface of nanoparticles, nanofibers, or within pores. Therefore, the development of new approaches and, based on them, functional polymer-containing composites to enhance the electro-physical and energy storage properties of power sources is one of the pathways to address global issues in this field.

This study thoroughly explores the energy storage characteristics of composites and coatings incorporating polymers. The research delves into the synthesis methods and underscores prospective pathways for applying these newly synthesized materials in energy storage and associated areas.



# Femtosecond Laser-Induced Periodic Surface Structures: Theory and Applications

I. Gnilitzkyi<sup>1,2\*</sup>

<sup>1</sup> Lviv Polytechnic National University, 12 Bandery Str., 79013, Lviv, Ukraine

<sup>2</sup> "NoviNano Lab" LLC, 5 Pasternaka, 79000, Lviv, Ukraine

\*Tel: (097) 170 9810, e-mail: [jaroslav.gnilitzkyi@novinano.com](mailto:jaroslav.gnilitzkyi@novinano.com)

Laser-induced self-organized structures, known as LIPSS, grooves, spikes, et al., represent a captivating phenomenon where high-intensity laser beams interact with various materials, giving rise to intricate surface patterns. These self-organized structures, characterized by periodic nano-microstructures, emerge spontaneously and have garnered significant attention due to their wide-ranging applications. This study delves into the formation mechanisms and the diverse practical uses of self-organised nano-microstructures.

The formation of LIPSS is a result of the complex interplay between intense laser pulses and the target material's surface. This interaction leads to the generation of plasma and subsequent energy redistribution, which, in turn, induces the spontaneous emergence of periodic surface structures. These structures exhibit ridges or grooves with dimensions in the order of the laser wavelength, giving them unique optical and physical properties. The practical applications of LIPSS are vast and continue to expand. Notable areas where these laser-induced structures have made significant strides include surface engineering, biomedical applications, high-density data storage, antibacterial surfaces, optics and photonics, superhydrophobic surfaces, and nanoscale materials.

In surface engineering, LIPSS have proven invaluable for enhancing materials' optical, mechanical, and thermal properties. By creating these structures on metal surfaces, for instance, their light-absorbing capabilities can be improved, making them crucial components in the realm of solar energy. LIPSS are also fighting the good fight against bacteria. By modifying material surfaces, these structures can prevent bacterial adhesion and growth, a critical development in healthcare settings.

Additionally, LIPSS can create superhydrophobic surfaces, which find use in self-cleaning coatings, anti-fog materials, and more. Their precision control over size and shape makes them pivotal in the development of nanoscale devices and sensors. Research in this field is ongoing, with scientists continuously exploring new materials and laser parameters to create tailored self-organized structures for specific applications. This research is fundamental to advancing our understanding of laser-material interactions and unlocking even more innovative applications.

In summary, laser-induced self-organized structures represent a mesmerizing fusion of fundamental science and practical applications. From surface engineering to biomedical advancements, data storage, and beyond, LIPSS is pushing the boundaries of what can be achieved with laser technology. As research in this field continues to evolve, we can expect even more innovative applications that leverage the self-organizing power of lasers to enhance various aspects of our lives.



## Comparison of Series and Shunt GaN RF Switches for Millimeter-Wave Applications

P. Bajurko<sup>1,2</sup>, J. Sobolewski<sup>1,2</sup>, Y. Yashchyshyn<sup>1,2\*</sup>

<sup>1</sup>Warsaw University of Technology, Nowowiejska 15/19, 00-665 Warsaw, Poland

<sup>2</sup>CENTERA Laboratories, Institute of High-Pressure Physics PAS, Sokołowska 29/37, 01-142 Warsaw, Poland

\*Tel: (4822) 234 77 27, e-mail: [yevhen.yashchyshyn@pw.edu.pl](mailto:yevhen.yashchyshyn@pw.edu.pl)

Modern radio frequency (RF) communication systems require high flexibility and the ability to adapt to changing operating conditions. One of the components essential to enable such properties are high-speed RF switches. Two main topologies of semiconductor switching devices can be distinguished [1]. First is a series switch, where an active element is used to interrupt the signal path and is placed between the input and output in series with the transmission line. It is a reflective type switch because, in the off state, the RF signal is reflected from the high-impedance active element [2]. The second topology is a shunt switch. In this type of device, the active element is used to create a short circuit to the ground in the transmission line. This is also a reflective type switch; however, as opposed to a series switch, the reflection is caused by the low impedance of the short circuit in the off state.

In this work, the suitability of both topologies for millimeter-wave (mm-wave) switch applications was analyzed. For comparison, several series and shunt switches were designed using the AlGaIn/GaN heterostructures, which allows the construction of high electron mobility transistor (HEMT) active elements. The GaN-based semiconductors are well suited for this application due to their high switching speed, high power handling capability, and ability to operate at high temperatures [3]. The switches were fabricated and examined in the frequency range from DC to 114 GHz.

The series switches exhibited a very high on/off ratio (30–50 dB) at low frequencies up to approximately 1–3 GHz, depending on the design. However, the insertion loss is relatively high, in the range from 3 dB to 5 dB. Above that frequency, the insertion loss and isolation degrade significantly. High insertion loss at low frequencies is a result of the significant series resistance of the transistor channel, while the degradation with frequency is caused by capacitive coupling between the transistor channel and the grounded gate. The degradation of isolation can be explained by fringe capacitances between source, drain and gate of the transistor. These issues make the series switches not well suited for mm-wave applications.

Although the shunt switches do not provide as high an on/off ratio at low frequencies as series constructions, they maintain reasonable values of this parameter across a very broad frequency range. In contrast to the series switch, on/off ratio increases with frequency from 14 dB at DC to above 22 dB at 114 GHz. The insertion loss is significantly lower than the values achieved by the series switches and slowly increases with frequency (from 1.9 dB at DC to 7.2 dB at 114 GHz). Shunt switches operate at DC and mm-wave frequencies at the same time, which is uncommon for RF switches and makes it suitable for a wide range of applications.

**Acknowledgment:** this work is part of a project IMAGE that has received funding from the European Union's Horizon2020 research and innovation programme under the Marie Skłodowska-Curie grant agreement No. 778156.

[1] J. Sobolewski, Y. Yashchyshyn, *IEEE ACCESS*, Vol. 10, 2022, pp. 12983–12999.

[2] Y. Yashchyshyn, et al., *Micromachines* 2021, vol. 12, no. 11, 1343.

[3] U. K. Mishra, P. Parikh, and Y. F. Wu, *Proc. IEEE*, vol. 90, no. 6, pp. 1022–1031, 2002.



## Why a Phosphor of the High Effective Atomic Number Can Be Useful for Dosimetry

S. Ubizskii<sup>1\*</sup>, O. Poshyvak<sup>1</sup>, Ya. Zhydachevskyy<sup>2</sup>

<sup>1</sup>Lviv Polytechnic National University, Stepan Bander St. 12, Lviv, 79013, Ukraine

<sup>2</sup>Institute for Physics, PAN, al. Lotników 32/46, Warsaw 02-668, Poland

\*e-mail: [Sergii.B.Ubizskii@lpnu.ua](mailto:Sergii.B.Ubizskii@lpnu.ua)

Since passive dosimetry is aimed at assessing the value of the absorbed dose as a measure of the possible impact of radiation on human health, one of the requirements for the dosimetric material used as a sensitive element is the equivalence of its absorption to that in human tissues. This property is determined by the effective atomic number  $Z_{eff}$  of the matter. A tissue-equivalent dosimetric material should have an effective atomic number close to 7.6, which is considered as a  $Z_{eff}$  averaged for the human tissues. In this case, the interaction of ionizing radiation with a matter occurs almost equally both in the material of the dosimeter and in the human body, and the same dosimeter calibrated for one radiation source with a certain energy will work correctly for radiation of other energies.

If the dosimetric material has a higher effective atomic number and is calibrated for one radiation energy, then the dose measured from its response to radiation of a different energy will be overestimated or understated depending upon energy and needs to be corrected. This can be done if the radiation energy is known. However, in the case of radiation accidents, the radiation energy and the type of source may not be known, or the dominant type of radiation is unknown if the radiation is mixed. This is the expected situation in the event of a terrorist attack using a so-called dirty bomb containing radioisotopes to contaminate the territory, air or water and expose people to radiation. In such case, it is necessary to assess not only the absorbed dose but also the type of radiation source itself, since an adequate response and treatment strategy in the event of radiation exposure of people depends not only on the absorbed dose but also on the type of exposure.

On the other hand, a dosimetric material that has a significantly higher  $Z_{eff}$  can solve the problem in some cases in a way that allows the difference in energy dependence of dosimetric sensitivity to be used to identify radioisotopes that are hazardous to external exposure. We report the results of analysis of the feasibility of such usage of high  $Z_{eff}$  dosimetric phosphor based on  $YAlO_3$  matrix ( $Z_{eff} = 31.4$ ) or  $LuAlO_3$  ( $Z_{eff} = 61.6$ ) in pair with almost tissue-equivalent dosimetric phosphor  $BeO$  ( $Z_{eff} = 7.1$ ) and requirements for "heavy" dosimetric material which can be used in such application as well as the implementation of the proposed approach.

**Acknowledgments:** This work was supported by the NATO SPS MYP program (project G5647), and by the Polish National Science Centre (project 2018/31/B/ST8/00774).



## Mercury Detection Sensor Based on the Structure of Amorphous Se Film/Au Nanoparticles

**M. Trunov\*, V. Rubish, V. Kyrylenko, M. Durkot**

*Uzhhorod Laboratory of Optoelectronics and Photonics Materials of the Institute for Information Recording, NAS of Ukraine, 4 Zamkovi Skhody str., 88000, Uzhhorod, Ukraine*

*\*Tel. (+380) 50 8032911, e-mail: [trunov.m@gmail.com](mailto:trunov.m@gmail.com)*

Mercury is a kind of toxic heavy metal, which widely exists in the form of mercury vapor, resulting in profound environmental repercussions and significant harm to human health. This is due to its chemical attributes, which encompass high toxicity, stability, bioaccumulation, persistence, long-range migration, and toxic Hg-based derivatives. Numerous methods for detecting mercury vapor have been employed, including conductometric, electrochemical, colorimetric, fluorescence, and biosensing technologies. Among the potential materials suitable for developing an active sensor element for detecting mercury vapor, amorphous Selenium has garnered considerable interest due to its altered physico-chemical properties upon exposure to mercury.

In our research, we propose utilizing the shift in the surface plasmon resonance (SPR) peak position within an amorphous Se film/Au nanoparticles structure. This shift occurs during the formation of HgSe nanocrystals on the surface of the Se film when exposed to Hg vapor. The suggested SPR sensor incorporates a layer designed to induce localized surface plasmon resonance, featuring a random distribution of Au nanoparticles, with a Se film layered on top.

To produce disordered arrays of gold nanoparticles (AuNPs) with particle sizes ranging from tens to hundreds of nanometers and an SPR peak between 520-597 nm, we applied rapid thermal annealing (30-60 seconds, 300-350 C) to gold film (4-35 nm thick) [1] on glass substrates. Additionally, amorphous selenium (Se) films, ranging from 5 to 50 nm in thickness, were fabricated by vacuum-evaporating vitreous Selenium onto glass substrates (nominal pure Se) and glass substrates covered by arrays of AuNPs (plasmonic structures). Transmission spectra were acquired using a fiber spectrophotometer (Ocean Optics). The SPR peak of the plasmonic structures closely matched the absorption range of amorphous Se (650-700 nm).

The modification of nominally pure Se films and plasmonic structures was carried out in a hermetic chamber at a temperature of 20°C. The concentration of mercury vapor in the air under these conditions was approximately 13.3 mg/m<sup>3</sup>.

The plasmonic structure exhibited high sensitivity to the presence of mercury vapor. The most sensitivity was observed for samples with a selenium film thickness less than 30 nm (5-15 nm). A 7 nm shift (633 nm to 640 nm) in the SPR maximum was reliably detected after 2 minutes of exposure. An exposure of 10 minutes resulted in a significant 32 nm shift (633-665 nm) with a simultaneous 20% decrease in transmission on the long-wave part of the SPR. Nominally pure selenium films of similar thickness showed only a slight change in transmission (around 1-2%), which was realistically detectable after 10 minutes of exposure.

In summary, our research confirmed that amorphous Se films, particularly those with a 5-15 nm thickness deposited on disordered AuNPs arrays, are more sensitive to mercury vapor than nominally pure Se films. Exposure of such plasmonic structures to mercury vapor led to a significant shift of the surface plasmon resonance into the long-wavelength region of the spectrum, with the maximum effect occurring at the initial exposure stage. Increasing the sensitivity of the sensor is possible with the use of micro/nanostructuring of the active element, for example, by direct optical formation of surface relief.

[1] V.M. Rubish et al. (2021) *Physics and Chemistry of Solid State*, 22, 804-810.



# Study of Relationship Between Nonlinear Optical Phenomena and the Molecular Structure of Specific Industrial Organic Compound

A. Aamoum<sup>1</sup>, S. Taboukhat<sup>2\*</sup>, A. Andrushchak<sup>3</sup>, R. Wielgosz<sup>4</sup>,  
M. Lelonek<sup>5</sup>, P. Göring<sup>5</sup> and B. Sahraoui<sup>2</sup>

<sup>1</sup>*Institute of Physics, Faculty of Physics, Astronomy, and Informatics, Nicolaus Copernicus University in Toruń, Grudziadzka 5, PL 87-100 Torun, Poland*

<sup>2</sup>*University of Angers, LPHIA, SFR MATRIX, 2 Bd. Lavoisier, 49045 Angers, France,*

<sup>3</sup>*Lviv Polytechnic National University, 12 S. Bandery str., 79013 Lviv, Ukraine*

<sup>4</sup>*Energia Oze Sp. z o.o., ul. Częstochowska 7, 42-274 Konopiska, Poland*

<sup>5</sup>*SmartMembranes, Heinrich-Damerow-Str. 4, Halle (Saale) 06120, Germany*

\*e-mail: [said.taboukhat@univ-angers.fr](mailto:said.taboukhat@univ-angers.fr)

Research into the nonlinear optical properties of organic compounds is rapidly growing and has a significant role in the emergence of photonic technologies. To develop innovative compounds for applications such as communication, optical switching, optical data storage, and optical limiting, advancements in materials based on the molecular engineering of sophisticated molecular systems displaying excellent nonlinear optical (NLO) responses are necessary [1,2]. Consequently, organic materials have been the focus of both experimental and theoretical investigations in recent years due to their promising potential in photonics and optical devices. There is a strong interest in the development of such photonic systems for applications in nonlinear optical and optoelectronic technologies [3].

The obtained results show the important nonlinear optical properties of the studied organic compound deposited as thin layers by using the Physical Vapor Deposition (PVD) and spin-coating techniques. The results provide concrete evidence that the studied selected organic compound presents a prospective candidate for producing optoelectronic devices.

**Acknowledgment:** the presented results are part of the IMAGE project that has received funding from the EU Horizon 2020 research and innovation program under the Marie Skłodowska-Curie grant agreement No 778156.

- [1] A. Aamoum, K. Waszkowska, S. Taboukhat, P. Płóciennik, M. Bakasse, Y. Boughaleb, J. Strzelecki, A. Korcala, Z. Sofiani, A. Zawadzka, *Opt Quant Electron.* 52 (2019).
- [2] S. Taboukhat, N. Kichou, J.-L. Fillaut, O. Alévêque, K. Waszkowska, A. Zawadzka, A. El-Ghayoury, A. Migalska-Zalas, B. Sahraoui, *Sci Rep.* 10 (2020) 15292.
- [3] J. Liu, C. Ouyang, F. Huo, W. He, A. Cao, *Dyes and Pigments.* 181 (2020) 108509.



## Selenium Thin Films Application in THz Range

A. Bendak<sup>1\*</sup>, I. Senko<sup>1</sup>, D. Vynnyk<sup>1</sup>, V. Rubish<sup>2</sup>

<sup>1</sup>Lviv Polytechnic National University, 12 S. Bandery, 79013 Lviv, Ukraine

<sup>2</sup>Institute for Information Recording, NAS of Ukraine, 4 Zamkovi Skhody, 88000 Uzhhorod, Ukraine

\*e-mail: [andrii.v.bendak@lpnu.ua](mailto:andrii.v.bendak@lpnu.ua)

It is well known that the research on THz technology has been an extremely rising scientific trend for the last decades. Several technical breakthroughs in electronics and photonics made since the early 1990s have started to bring terahertz (THz)-wave technologies from laboratory demonstrators to industrial applications such as non-destructive testing, security, medicine, communications, etc. [1]. Therefore, developing THz-controlling devices is a promising task, including searching and preparing new materials and innovative construction technologies. Within the framework of the set of problems, we will consider the basic principles of optically controlled devices for THz irradiation. Generally, the influence of illumination on photosensitive semiconductors is proposed as an essential phenomenon used for the desired result.

It should be noted that a number of scientific works deal with research on optically controlled devices. An expected innovation contains quality improvement, efficiency, miniaturization, etc. Despite the reliable physical properties of selected materials, their modification would have promising results. In particular, a transition from 3D bulk to 2D systems – thin films and 1D – nanotubes, nanopillars. For example, another modification method remains doping or surface morphology changes [2,3].

Assuming the mentioned above, we will discuss Selenium thin films as a promising material for THz devices investigation. Since photoconductive properties and high photosensitivity of Selenium are well established and studied, there is a need to perform experimental work to investigate Volt-Ampere characteristics of Se thin-film under illumination in the framework of our current research (Fig. 1). To confirm the possibility of Se thin-films application in the given task it was decided to study their properties under illumination with different wavelengths and intensities. Such experimentally obtained properties should present a more detailed view of assigned tasks.

**Acknowledgments:** This work has received funding from the National Research Foundation of Ukraine (Project 2021.01/0410).

[1] T. Nagatsuma (2011) *IEICE Electronics Express*. 8(14), 1127-1142.

[2] B. Hou et. al. (2010) *Proc. SPIE 7854, Infrared, Millimeter Wave, and Terahertz Technologies*, 785405.

[3] Q.-Y. Wen et. al. (2020) *Adv. Mater. Technol.* 5, 1901058.

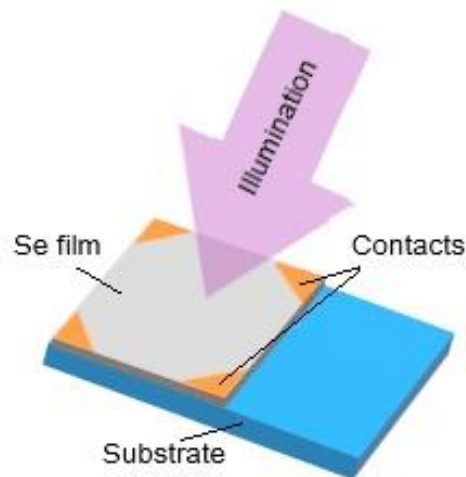


Fig. 1. Illustrative drawing of Selenium thin-film deposited onto quartz substrate. Changes of Volt-Ampere characteristics of thin-film under illumination represents investigated experiment.